NAVAL POSTGRADUATE SCHOOL

MONTEREY, CALIFORNIA

THESIS

HYDROGEN FUEL OPERATION FOR GAS TURBINE ENGINES

by

Ethan J. Hardt

June 2021

Thesis Advisor:	Anthony J. Gannon
Co-Advisor:	Garth V. Hobson
Second Reader:	Walter Smith

Approved for public release. Distribution is unlimited.

THIS PAGE INTENTIONALLY LEFT BLANK

REPORT DOCUMENTATION PAGE	*Form Approved OMB No. 0704-0188*

1. AGENCY USE ONLY ***(Leave blank)***	**2. REPORT DATE** June 2021	**3. REPORT TYPE AND DATES COVERED** Master's thesis

4. TITLE AND SUBTITLE HYDROGEN FUEL OPERATION FOR GAS TURBINE ENGINES	**5. FUNDING NUMBERS** RMNPB
6. AUTHOR(S) Ethan J. Hardt	
7. PERFORMING ORGANIZATION NAME(S) AND ADDRESS(ES) Naval Postgraduate School Monterey, CA 93943-5000	**8. PERFORMING ORGANIZATION REPORT NUMBER**
9. SPONSORING / MONITORING AGENCY NAME(S) AND ADDRESS(ES) Office of Naval Research, Arlington, Virginia.	**10. SPONSORING / MONITORING AGENCY REPORT NUMBER**

11. SUPPLEMENTARY NOTES The views expressed in this thesis are those of the author and do not reflect the official policy or position of the Department of Defense or the U.S. Government.

12a. DISTRIBUTION / AVAILABILITY STATEMENT Approved for public release. Distribution is unlimited.	**12b. DISTRIBUTION CODE** A

13. ABSTRACT (maximum 200 words)

The purpose of this thesis was to operate a gas turbine engine on hydrogen fuel at near full load. Hydrogen fuel is sought after by the Department of the Navy due to its ability to increase energy security and energy independence to naval forces. The two engines researched were the C30 Capstone microturbine and JetCat P60 turbine. The Capstone C30 was experimentally run with hydrogen fuel and these results are compared to propane fuel data at varying loads. The JetCat P60 was simulated using a hydrogen fuel source. These simulations aid in potential engine modifications to ensure safe operation for future experimental work. Recommendations to produce a fully operational hydrogen supply system are discussed as well as to operate the C30 at full power.

14. SUBJECT TERMS hydrogen, micro turbine, energy, renewable energy	**15. NUMBER OF PAGES** 99
	16. PRICE CODE

17. SECURITY CLASSIFICATION OF REPORT Unclassified	**18. SECURITY CLASSIFICATION OF THIS PAGE** Unclassified	**19. SECURITY CLASSIFICATION OF ABSTRACT** Unclassified	**20. LIMITATION OF ABSTRACT** UU

NSN 7540-01-280-5500 Standard Form 298 (Rev. 2-89) Prescribed by ANSI Std. 239-18

THIS PAGE INTENTIONALLY LEFT BLANK

HYDROGEN FUEL OPERATION FOR GAS TURBINE ENGINES

Ethan J. Hardt
Ensign, United States Navy
BS, United States Naval Academy, 2020

Submitted in partial fulfillment of the
requirements for the degree of

MASTER OF SCIENCE IN MECHANICAL ENGINEERING

from the

NAVAL POSTGRADUATE SCHOOL
June 2021

Approved by: Anthony J. Gannon
Advisor

Garth V. Hobson
Co-Advisor

Walter Smith
Second Reader

Garth V. Hobson
Chair, Department of Mechanical and Aerospace Engineering

THIS PAGE INTENTIONALLY LEFT BLANK

ABSTRACT

The purpose of this thesis was to operate a gas turbine engine on hydrogen fuel at near full load. Hydrogen fuel is sought after by the Department of the Navy due to its ability to increase energy security and energy independence to naval forces. The two engines researched were the C30 Capstone microturbine and JetCat P60 turbine. The Capstone C30 was experimentally run with hydrogen fuel and these results are compared to propane fuel data at varying loads. The JetCat P60 was simulated using a hydrogen fuel source. These simulations aid in potential engine modifications to ensure safe operation for future experimental work. Recommendations to produce a fully operational hydrogen supply system are discussed as well as to operate the C30 at full power.

THIS PAGE INTENTIONALLY LEFT BLANK

TABLE OF CONTENTS

LIST OF FIGURES

LIST OF TABLES

THIS PAGE INTENTIONALLY LEFT BLANK

LIST OF ACRONYMS AND ABBREVIATIONS

C30	Capstone Turbine Corporation C30 Microturbine
CFD	computational fluid dynamics
DOD	Department of Defense
DON	Department of the Navy
FOD	foreign object debris
HAZ	heat affected zone
K	Kelvin
kN	kilonewton
kPa	kilopascal
kW	kilowatts
m/s	meters per second
PSFC	power specific fuel consumption
RPM	revolutions per minute
s	seconds
TET	turbine exit temperature
TSFC	thrust specific fuel consumption

THIS PAGE INTENTIONALLY LEFT BLANK

ACKNOWLEDGMENTS

I would like to thank my family and friends for their support during my studies at NPS and USNA. I would like to thank USNA professors, LCDR Ethan Lust and Professor Patrick Caton, for mentorship and encouragement to continue my education at NPS.

I would like to thank Dr. Anthony Gannon and Dr. Garth Hobson for the vision of this hydrogen project. Dr. Walter Smith for teaching me about the operation of the C30 system, and lastly, Mr. John Gibson for technical support while working with the engines.

THIS PAGE IS INTENTIONALLY LEFT BLANK

I. INTRODUCTION

The purpose of this research is to extend the work of developing hydrogen-fueled gas turbine engines. Hydrogen engines have potential to revolutionize the renewable energy needs of the Department of the Navy (DON). This work is sponsored by the Office of Naval Research. The objectives of this research are to reconfigure a Capstone Turbine Corporation C30 Microturbine (C30) for hydrogen operation, evaluate parameters affected by different sources of fuel, and model hydrogen fuel combustion in a JetCat P60 engine.

A. MOTIVATION

Renewable energy is one of the fastest growing energy sources globally. Private businesses and federal governments are developing new technology in order to gain energy independence from oil and natural gas. Within the U.S. federal government, the DON is a front runner in researching renewable energy. One reason is because over 80 percent of the federal government's energy consumption occurs within the DON [1]. The DON also has two major energy goals: energy security and energy independence [2]. Energy security is "the ability to protect and deliver sufficient energy to meet all operational needs" [2]. Energy independence is relying only on energy sources that can withstand accidental or intentional disruptions. It also "increases operational effectiveness by making Naval forces more *energy self-sufficient* and less dependent on vulnerable energy production and supply lines" (emphasis added) [2].

Along with the DON search for a renewable energy strategy, the Department of Defense (DOD) is looking for a solution to counter attacks on energy logistics. "Between Oct 2001 and Dec 2010, 52% of Operation Enduring Freedom and Operation Iraqi Freedom casualties occurred from hostile attacks during land transport missions" [3]. The DON has also encountered casualties with refueling like the attack on the USS Cole. The DOD and DON want a fuel source that lasts longer and can be produced through renewable energy.

The fuel source of interest is hydrogen. Hydrogen combustion in air is similar to typical hydrocarbons used in gas powered turbines. Unlike propane and methane, which produce carbon dioxide in reactions with air, hydrogen primarily produces water and little or no carbon dioxide. A hydrogen and air reaction is a carbon free reaction desired for the DON renewable energy initiative.

B. LITERATURE REVIEW

Hydrogen is a unique fuel source because of its extremely high gravimetric density compared to other fuels such as methane and JP-8. Combined with being the most abundant and simplest element, the small and light molecular structure has potential to be the future of renewable energy.

The primary way to produce hydrogen is through gasification. Breaking hydro-carbon bonds allows for hydrogen to be extracted in large quantities for reasonable costs and high efficiency. Issues occur in the byproducts of this process by omitting CO and CO_2 [4]. An alternative way to produce hydrogen is electrolysis. Electrolysis is used to separate water into hydrogen and oxygen. Once separated, hydrogen is then compressed and stored. The small process means it can be applied practically anywhere around the world since only electricity and water is required. While the process is easy to apply, high production costs due to low conversion efficiency and electrical power are major drawbacks to large scale production [5]. However, combined with emission free electricity, such as wind, solar, or geothermal power, hydrogen can become a renewable fuel cell.

The difficulty in using hydrogen comes from the low volumetric density. Figure 1 is a comparison of gravimetric and volumetric density of different fuels.

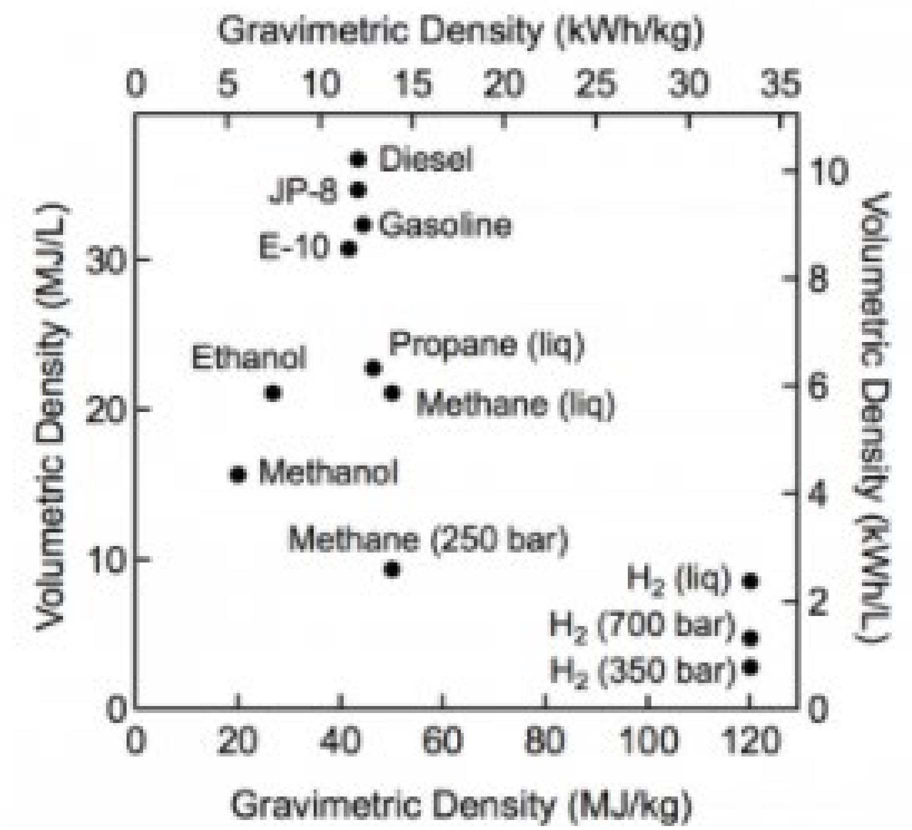

Figure 1. Comparison of gravimetric density and volumetric density based on LHV

Hydrogen at ambient pressure only has 0.0107 MJ/L, which is three times smaller than methane and almost 2500 times smaller than liquid propane [5]. The low volumetric density has often been the reason hydrogen was avoided as an alternative fuel.

Another issue which arises is the compression and storage of hydrogen. Currently, hydrogen is compressed into high pressure vessels. The main problem with this approach is hydrogen's low storage density [5]. The low storage density requires hydrogen fuel to be stored in large, high pressure canisters compared to methane and propane fuel tanks. There will be difficulty in overcoming the storage problem of hydrogen, but these problems can be overcome with recent renewed interest in hydrogen.

C. PREVIOUS WORK

Kaufmann [6] worked with the Capstone C30 Microturbine. Kaufmann modeled CFD combustion, but only for a general combustion chamber. The three fuels compared were propane, methane, and hydrogen. The findings of this simulation showed that hydrogen had an adiabatic flame temperature almost 400 K higher than propane and methane. This showed that a new hydrogen combustion chamber may have to be created to replace the original propane and methane combustion chamber in order to deal with the higher increase in temperature. Another potential issue with the hydrogen fuel is the ability to supply the required volumetric flow rate. Kaufmann then analyzed the C30 itself. The C30 was run on propane, natural gas, and lastly, hydrogen. Propane and natural gas were able to fully operate the C30 on idle speed. Hydrogen was only able to run on idle speed for a short duration. Kaufmann’s test results for engine speed and turbine exit temperature (TET) are shown in Figure 2.

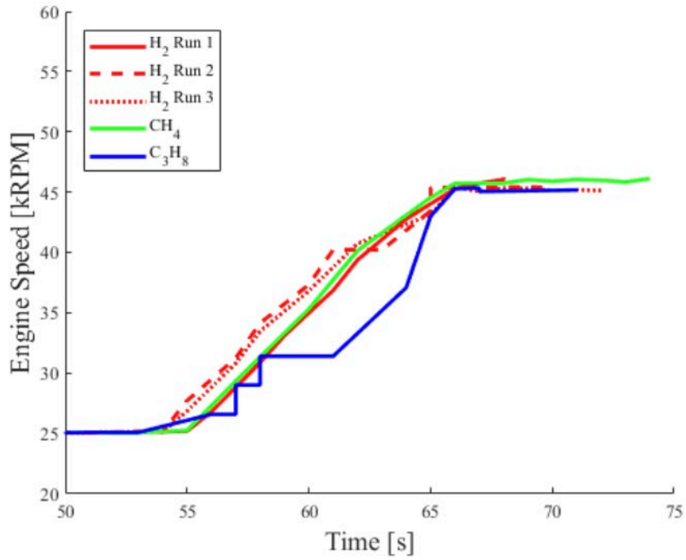

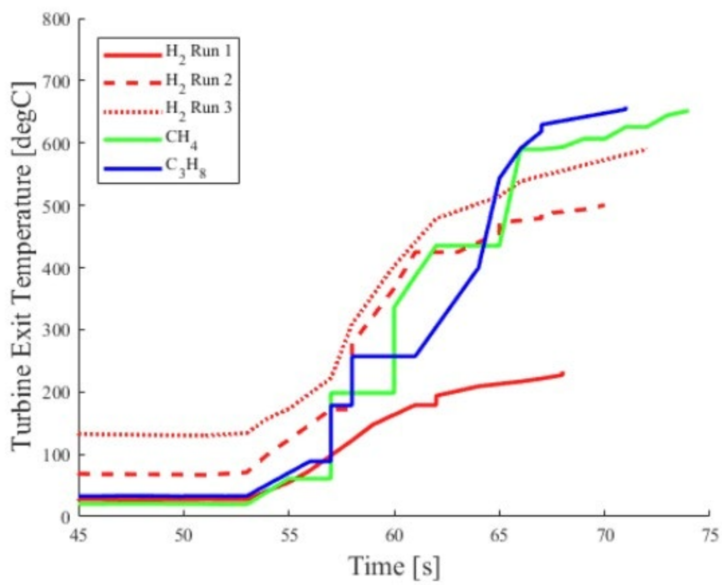

Figure 2. C30 Capstone test results for engine speed and TET for different fuel sources. Source: [6].

Three different runs used hydrogen but at different input pressures. The higher the input pressure increased the run time. One issue noted was the potential choked flow in the hydrogen line to prevent higher pressures from having sustained combustion.

D. APPROACH

This thesis analyzed the use of hydrogen fuel in two different engines. The two engines analyzed were the C30 Capstone and JetCat P60. The C30 Capstone is a larger engine capable of providing 30 kW of power, while the JetCat, a remote control plane turbofan engine, produces around 63 N of thrust. The C30 was chosen as the experimental engine because of its tested ability by its manufacturer to operate on hydrogen fuel [6]. The experimental test compared the use of hydrogen fuel and propane fuel at similar operating conditions. Once the data was captured and processed for a variety of different operating conditions, GASTURB simulations were generated to calculate fuel flow rates and other parameters which were unable to be measured during the experimental testing. The JetCat hydrogen operation is unknown because the engine was designed to burn liquid fuel. The JetCat engine was simulated at operating conditions using computational fluid dynamics (CFD). The simulation was intended to identify areas for combustion chamber modifications for safe and successful experimental research.

Recommendations were made to improve the hydrogen fuel supply line for the C30. JetCat recommendations included different modeling techniques to best model actual combustion within the combustion chamber. Future work can lead to implementation of hydrogen capturing systems to create fuel cells capable of running and refueling the C30 within the same system.

II. C30 DESIGN MODIFICATIONS

Modifications were made to the previous experimentational setup of the C30, a 30 kW electrical generating gas turbine. The two primary design modifications were involved with safe operation of the Capstone engine and additional testing equipment for further experimental results. The setup for the propane and hydrogen systems are shown in Figure 3.

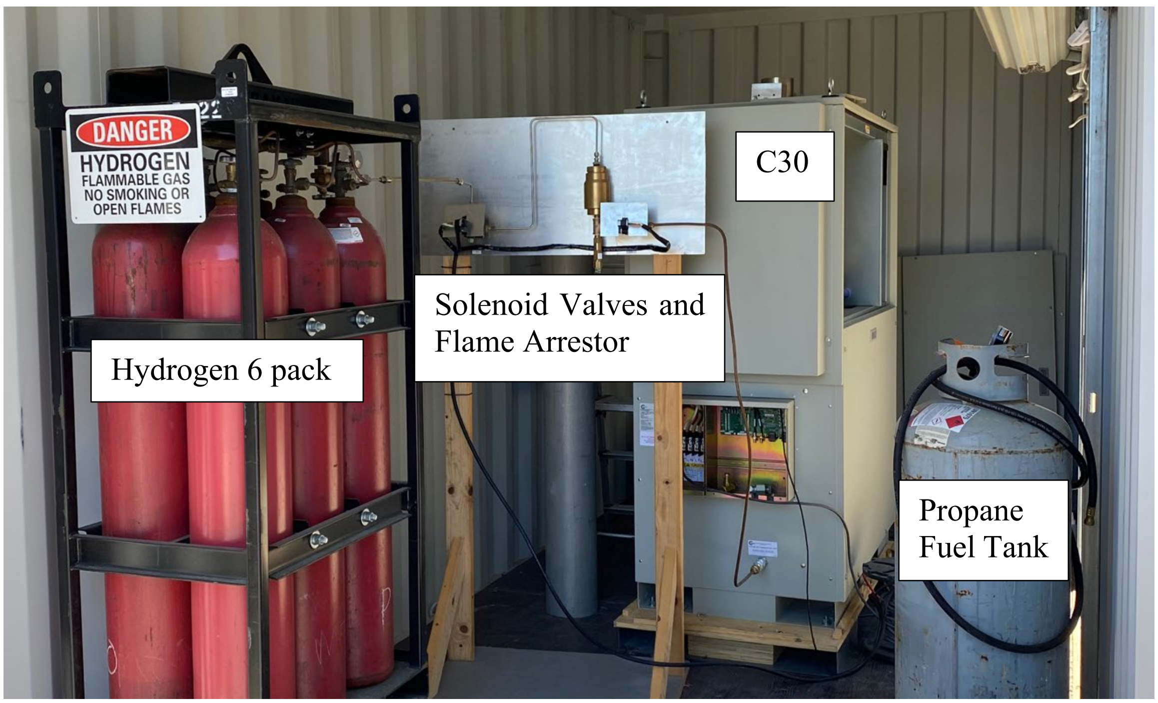

Figure 3. Propane and hydrogen fuel supply systems

The propane system on the right contains a propane filled tank with a regulator and a 9.52 mm flexible fuel line. The hydrogen system on the right contains a 6 pack of fuel tanks with a regulator, two solenoid valves, a flame arrestor, and 6.35 mm fuel tubing. The fuel supply systems and the C30 were all stored in a conex box shown in Figure 4.

Figure 4. Conex box for C30 and fuel supply system

A. CAPSTONE COMBUSTION CHAMBER

Capstone, the engine manufacturer, recommended the removing and capping of three pre-mix injectors from the combustion chamber [7]. The original combustion chamber and the modifications are shown in Figures 5 and 6.

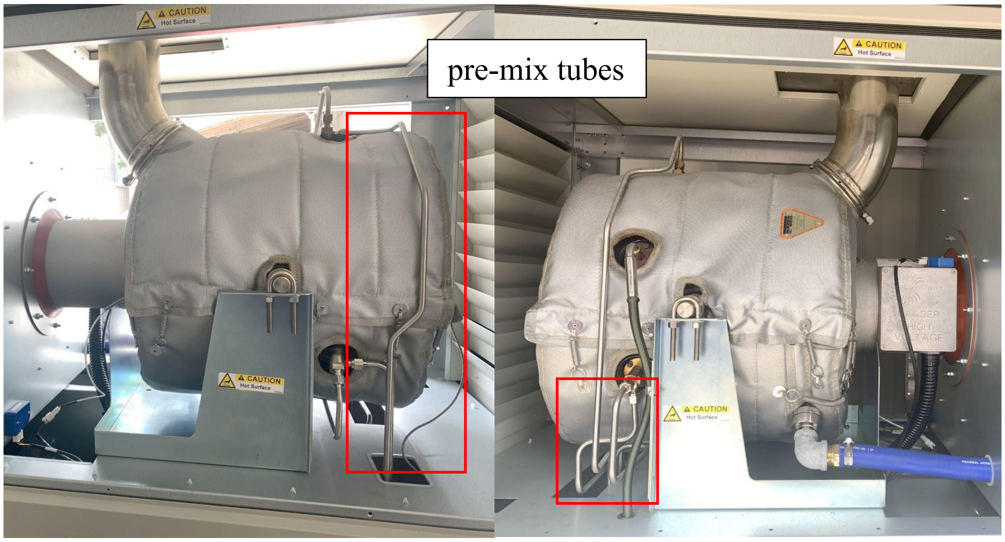

Figure 5. Original combustion chamber with pre-mix tubes.

Figure 6. Combustion chamber without pre-mix tubes and capped fittings.

These injectors were removed to reduce the risk of injector flashback. Flashback is burning in the injector which travels toward the fuel source. The hydrogen's higher flame speed increases the risk of injector flashback within the Capstone engine [7]. Injector flashback has potential to melt the fuel injectors leading to foreign object debris (FOD) to the turbine rotor.

A future design modification would be to place valves at the pre-mix injectors. The purpose of these valves would be to easily switch between a hydrogen and propane fuel source. The pre-mix tubes would also need modifications to fit with the added valves.

B. ADDITIONAL TESTING EQUIPMENT

A Mosebach's X30 load bank was added to the system to test the C30 at full power. The load bank applied loads for different operating conditions of the C30. The C30 was able to record and capture the data from the applied loads. The load bank and its connection to the Capstone engine are shown in Figure 7.

Figure 7. Load bank and end connection to C30.

The load bank allows for loads varying form 1 kW up to 30 kW [8]. The dials contain one 1 kW switch, two 2 kW switches, one 5 kW switch, and two 10 kW switches. The power supply can be easily varied throughout an experimental run to collect data at different output power levels. Turning on all switches represents 30 kW and the maximum power the C30 Capstone can supply. The four connections are applied directly to the Capstone engine along with a ground connection, far left.

C. PROPOSED FUTURE SUPPLY DESIGN

Following the experimental runs of the C30, the engine fuel inlet pressure was observed to decrease during the loaded hydrogen runs. A lower inlet pressure was expected due to a potential choked flow in the 6.35 mm fuel tubing because of hydrogen's low volumetric density shown in Figure 1. It is almost 4 times smaller than propane's volumetric density. The lower volumetric density implies the need for increased fuel tube sizing to increase overall mass fuel flow. Although the input pressure was expected to drop, the data showed a continual decrease in inlet pressure as the applied load increased. The C30 was unable to operate off 30 kW due to a low input fuel pressure. To avoid future problems with low fuel inlet pressure, a new hydrogen supply system was designed. The hydrogen system still contains essential safety features including two solenoid valves and a flame arrestor. The updated hydrogen supply system is shown in Figure 8.

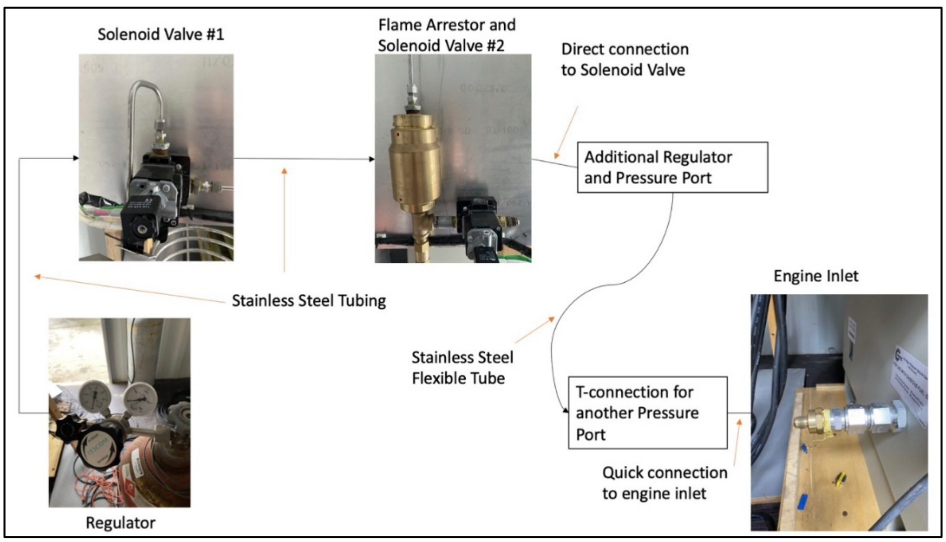

Figure 8. Updated hydrogen supply system/design

The main features added to the supply system are increased tubing sizes, from 6.35 mm to 9.52 mm, an additional flow regulator, pressure port connections, and a quick release system. The tubing sizes were increased because choked flow was assumed, due to the drastic decrease in pressure drop. The regulator was added to decrease the high back pressure after the hydrogen has traveled through the solenoid valves and flame arrestor. The pressure port connections will be used to measure the pressure throughout the system to determine where pressure drop is occurring. The quick release system was added to efficiently change between fuel sources.

THIS PAGE INTENTIONALLY LEFT BLANK

III. OPERATION OF C30 CAPSTONE

The high-pressure C30 Capstone was used for both propane and hydrogen fuel. The original fuel supply systems for the propane and hydrogen were not altered. The C30 operating procedure can be found in Appendix A. The two fuels were able to successfully run the C30. The comparisons between the two fuels are shown through tables and plots for variable loading conditions. GASTURB, a gas turbine simulation program, was also used to aid in comparing parameters for which the C30 did not have the instrumentation to measure.

A. RESULTS AND ANALYSIS

The main parameters measured by the C30 were engine speed and TET. Engine speed was selected to verify steady state operation when transitioning between applied loads. TET is measured to have an additional parameter to set up simulation data for comparisons. Table 1 shows a comparison between propane and hydrogen while under idle operation.

Table 1. C30 test results for idle operation

Fuel	Propane	Hydrogen
Input Pressure [kPa]	345	690
Fuel Valve Inlet Pressure [kPa]	343	640
Steady State TET [K]	949	952

The input pressure is the pressure specified at the exit of the fuel tank. The fuel valve inlet pressure is the pressure measured by the engine after flowing through the fuel lines. Although hydrogen has an input pressure two times larger than propane, the steady state TET’s remain nearly the same. This is expected because of the removal of the three mixing tubes of the combustion chamber, and the engine control system which varies the amount of fuel to a set operating point. Hydrogen has only three points of entry while propane has six. To overcome the lack of mixing tubes, the hydrogen needs a higher input pressure.

1. Propane Fuel

Propane had an input pressure regulated to 345 kPa. This pressure was chosen because of the prior experiments conducted by Kaufmann on the high pressure C30 [6]. The C30 was able to easily transition between 5 kW – 30 kW. Figures 9 and 10 display engine speed and TET at varying loads.

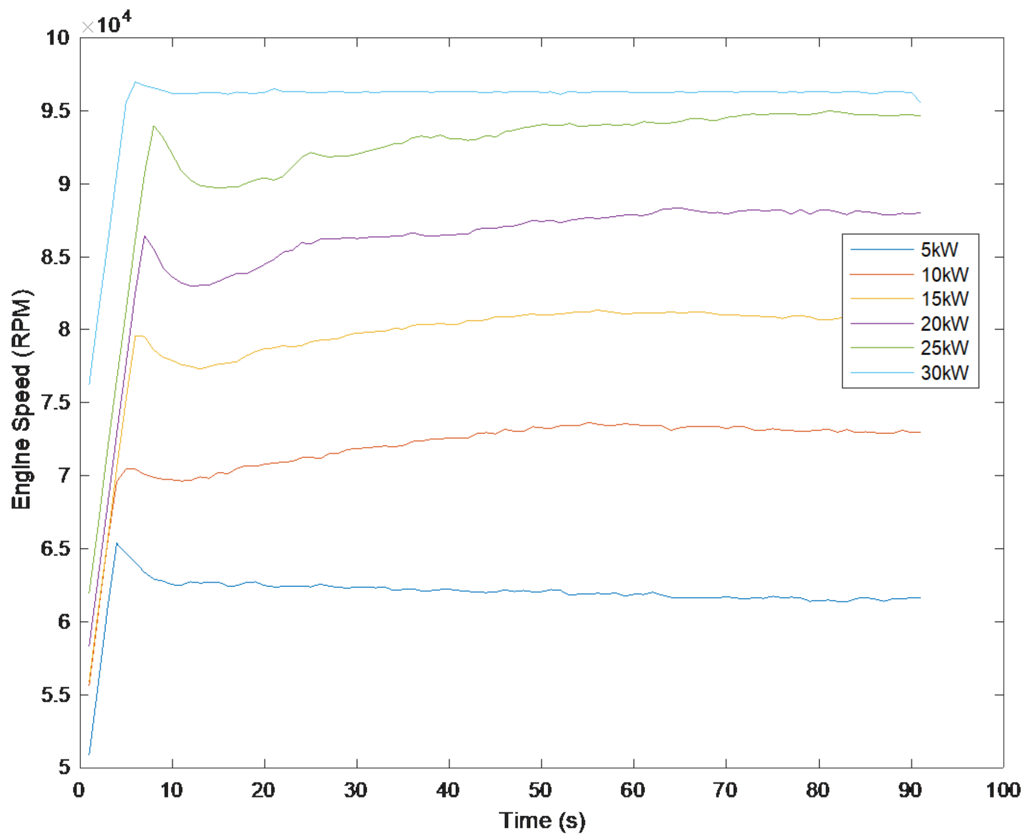

Figure 9. Engine Speed versus time for varying load propane fuel

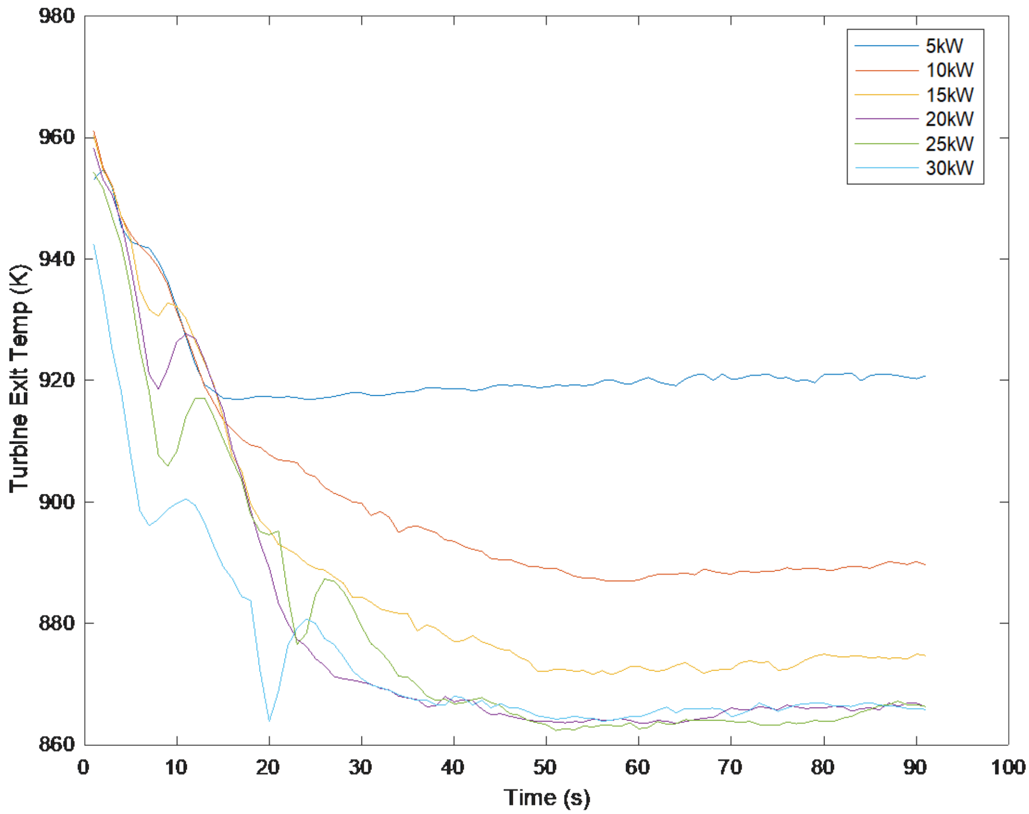

Figure 10. Turbine exit temperature versus time for varying load propane fuel

The C30 was able to reach steady state TET after 40 seconds for all of the trials. The inlet pressure remained constant through the different loads, and the steady state TET slightly decreased as the load increased. This occurred because the engine control system ensured a steady supply of fuel was inputted into the engine to obtain desired operating conditions. Table 2 shows the input pressure, inlet pressure, and steady state TET.

Table 2. C30 test results for propane variable loads

Load [kW]	5	10	15	20	25	30
Input Pressure [kPa]	345	345	345	345	345	345
Fuel Valve Inlet Pressure [kPa]	275	275	275	275	275	275
Steady State TET [K]	965	961	963	961	958	942

2. Hydrogen Fuel

Initial hydrogen testing consisted of three runs with input pressures of 276 kPa, 517 kPa, and 690 kPa with a goal of achieving idle operation. The engine ran for around 20 seconds on both the 276 kPa and 517 kPa runs. The engine entered shutoff mode soon after ignition due to low fuel inlet pressure. The engine was only reading around 35–55 kPa inlet pressure even though the system was set to give 276 kPa and 517 kPa. The last idle trial consisted of increasing the input pressure to 690 kPa. The engine successfully ignited and ran until it was intentionally shut-down because of a low fuel supply.

A six pack of hydrogen fuel was then added to the fuel supply to increase run time capability. The input pressure was set to 690 kPa and run with the load bank applied. The C30 was run at loads of 5 kW, 15 kW, 20 kW, and 25kW. Additional runs were conducted for repeatability of the experiment. The engine speed and TET are displayed against run time in Figures 11 and 12.

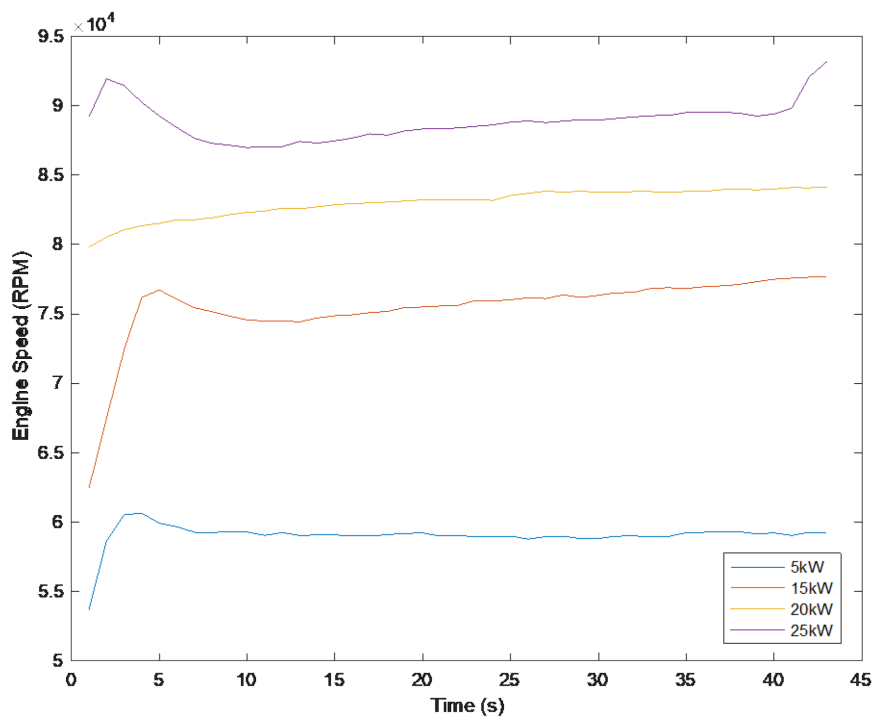

Figure 11. Engine Speed versus time for varying load hydrogen fuel

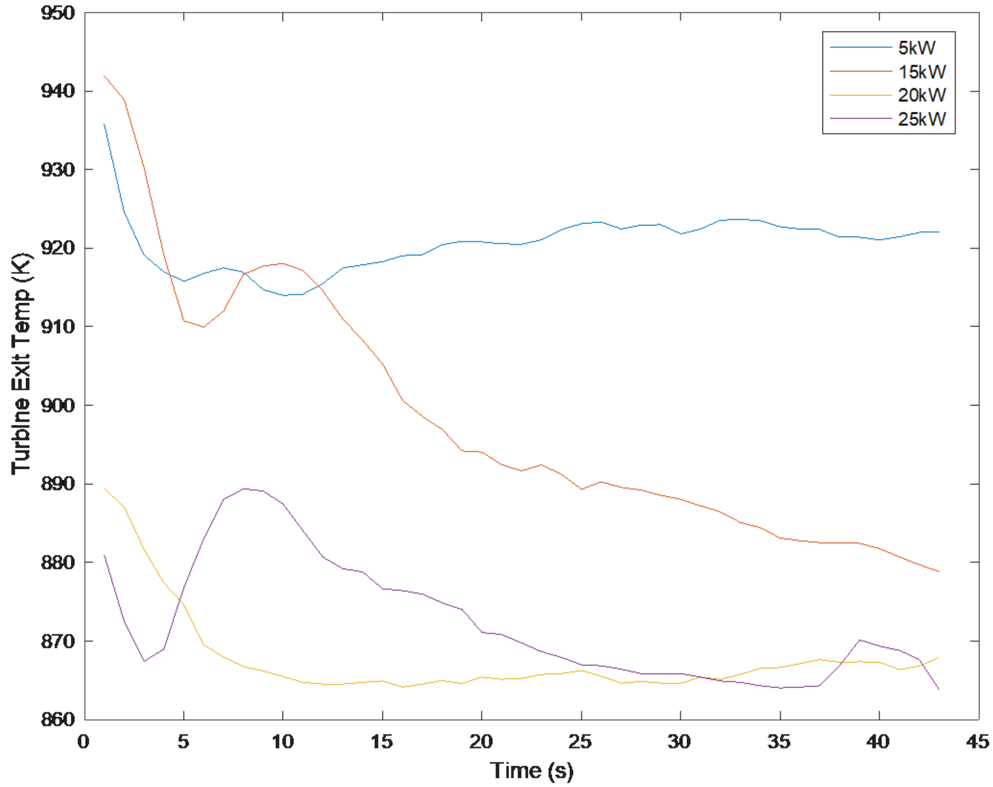

Figure 12. Turbine exit temperature versus time for varying load hydrogen fuel

The data collected was similar to expected results. The repeated runs show similar results. The 15 kW and 25 kW was not fully converged when the load was switched. The engine was easily able to transition between 5 kW – 25kW loads. Similar to the propane fuel, the TET lowered as the power demanded increased. Table 3 displays the values of input pressure, inlet pressure, steady state TET for hydrogen at different loads.

Table 3. C30 test results for hydrogen variable loads

Load [kW]	5	15	20	25
Input Pressure [kPa]	690	690	690	690
Fuel Valve Inlet Pressure [kPa]	607	552	525	469
Steady State TET [K]	936	942	932	932

Although the input pressure remained constant throughout the run, the inlet pressure decreased at each increase in load. The inlet pressure is the average pressure seen during the run. The pressure did slowly rise throughout the run which could possibly lead to the inlet pressures reaching closer to 690 kPa, but it would take an extended period of time to reach this high of a pressure. One attempt was made to run at 30 kW but was unsuccessful due to a low fuel inlet pressure. Recommendations for higher load runs are mentioned in the conclusions.

B. GASTURB COMPARISON

Although propane is not a preset fuel for a one spool turboshaft, turboprop engine simulation in GASTURB, generic fuel is an acceptable substitute because of the similar fuel heating value. Experimental data was set as parameters in GASTURB in order to accurately model the C30 engine. Adjustments were made to the simulated engine's compressor efficiency, turbine efficiency, and combustion chamber exit temperature to match the inlet pressure, TET, and shaft power of the experimental data at 30 kW.

After propane was simulated, the same engine setup was used to model a hydrogen fuel at 30 kW. The only differences, besides the fuel source, were the burner efficiency and the burner pressure ratio, which decreased by 0.1 and 0.01, respectively. GASTURB inputs and outputs can be found in Appendix B.

Off design calculations were performed to compare simulated data to experimental data at different loads. To more accurately simulate the C30 engine, different compressor maps were analyzed against the experimental data. Experimental data is plotted against GASTURB data from a standard axial compressor map and a DLR radial compressor map. The radial compressor map was chosen because the C30 operates with a radial compressor. These plots are displayed in Figures 13 and 14.

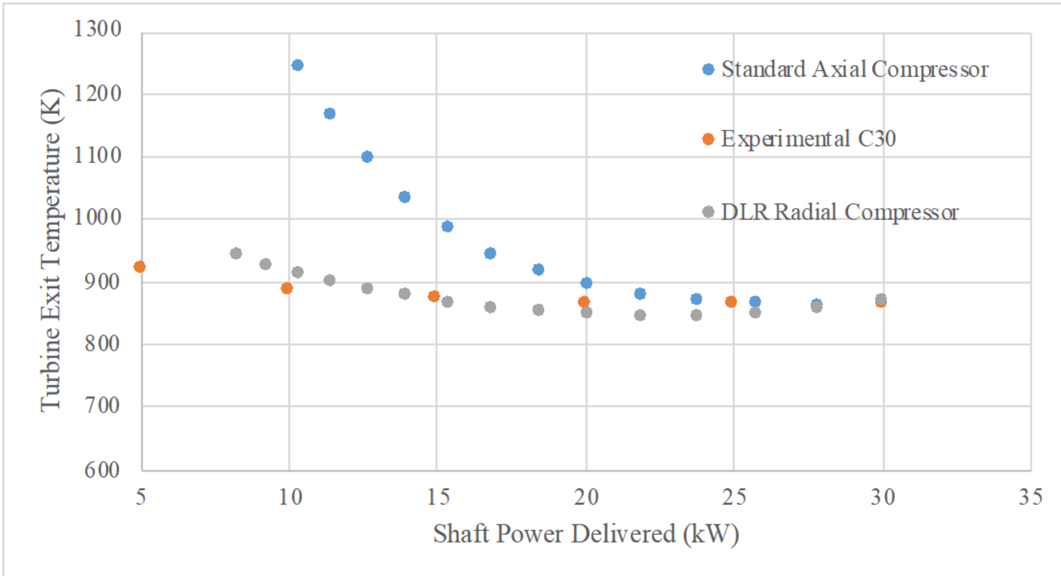

Figure 13. Comparison of GASTURB and experimental turbine exit temperature at different loads for propane fuel

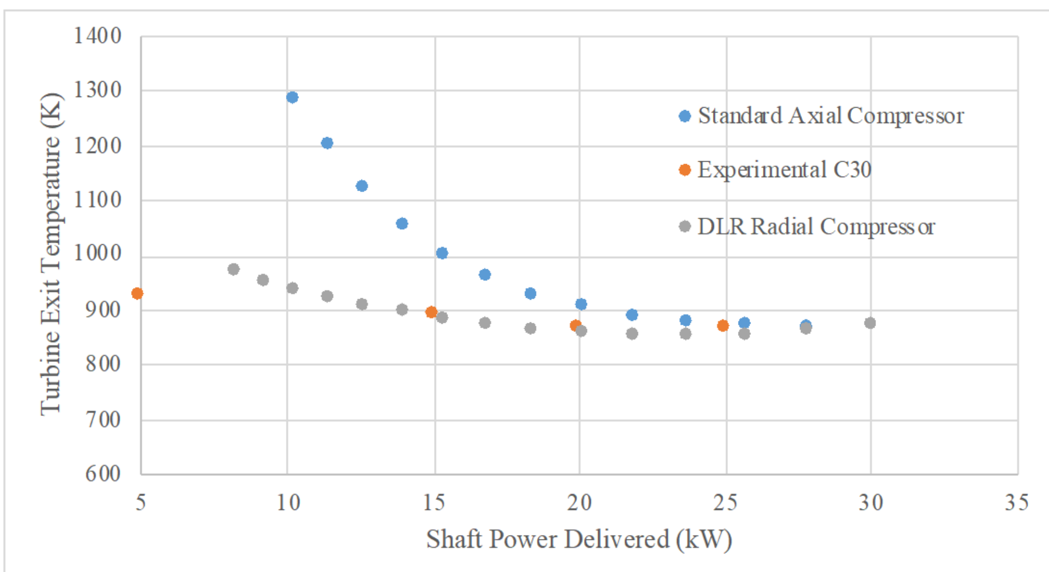

Figure 14. Comparison of GASTURB and experimental turbine exit temperature at different loads for hydrogen fuel

Altering compressor maps does not have much effect on operation between 25–30 kW. The difference is noticed when operating at conditions less than 25 kW. The standard compressor map TET has a larger error than the DLR map for the different operating loads.

Two additional parameters were compared. Those parameters were fuel mass flow rate and power specific fuel consumption. To compare the mass flow rates, the pressure readings of the hydrogen 6 pack were recorded during the runs. The recordings consisted of pressure readings before and after each load was applied. A sample of these calculations and a table of the calculated values can be found in Appendix C. The sample calculations had fuel mass flows varying from 0.0008 to 0.001 kg/s compared to the GASTURB value of approximately 0.0009 kg/s. The GASTURB values are well within the range of the experimental values. More accurate measurements can be implemented in the future to determine exact values at the different applied loads.

The final comparison analyzed was the power specific fuel consumption (PSFC). At max power of 30 kW, the hydrogen fuel has a PSFC of 0.124 kg/(kW-h). Propane fuel has a PSCF of 0.283 kg/(kW-h). Table 4 displays the PSFC comparison at different loads.

Table 4. Power specific fuel consumption for C30

Load [kW]	20	25	30
Propane [kg/(kW*h)]	0.2992	0.2879	0.2830
Hydrogen [kg/(kW*h)]	0.1397	0.1300	0.1242

Hydrogen will use less than half of the weight in fuel than propane for the same operating power and duration. These power specific fuel consumption values were taken from the data set using dlrrad compressor maps.

C. DISCUSSION AND RECOMMENDATIONS

It is hypothesized that hydrogen is an alternative, renewable fuel of the future. The experimental research of the C30 has led to valuable insight on the possibility large scale renewables for the DON. The experimental data was able to validate the simulated GASTURB data. The simulated data allowed for additional parameters to be extracted from the experimental results. Off design parameters were reliable from 15 kW and greater.

Although a new hydrogen supply system is recommended, the experimental results show that sustained hydrogen operation under load is possible. Only slight modifications need to be made to the C30. These modifications are there to increase the safety of hydrogen fuel use by decreasing the chances of flash back. A large-scale facility would be able to operate off a single C30 with hydrogen fuel provided a steady supply of fuel was available.

The proposed hydrogen supply system should be implemented, when possible, to improve the volumetric flow rates at lower input pressures. The system design will be easy to incorporate to the existing supply lines and better improve measurements for future experimental runs. Additionally, gas valves should be placed on the pre-mix tubes for easy conversion from hydrocarbon to hydrogen fuel. The C30 is versatile enough to meet the demands of both a hydrocarbon and hydrogen fuel source.

THIS PAGE INTENTIONALLY LEFT BLANK

IV. JETCAT SIMULATIONS

The JetCat engine was designed to have initial combustion with propane fuel followed by continued operation off kerosene. Because of the two different properties of the fuels, gas and liquid, CFX modeling was implemented to gain a better understanding of a purely gaseous operation. Hydrogen fuel was the only fuel analyzed using CFX.

A. MODELING

The exact JetCat combustion chamber was not modeled. Instead, a close replica solid model of the combustion chamber was obtained [9]. The model and actual combustion chamber are shown in Figure 15.

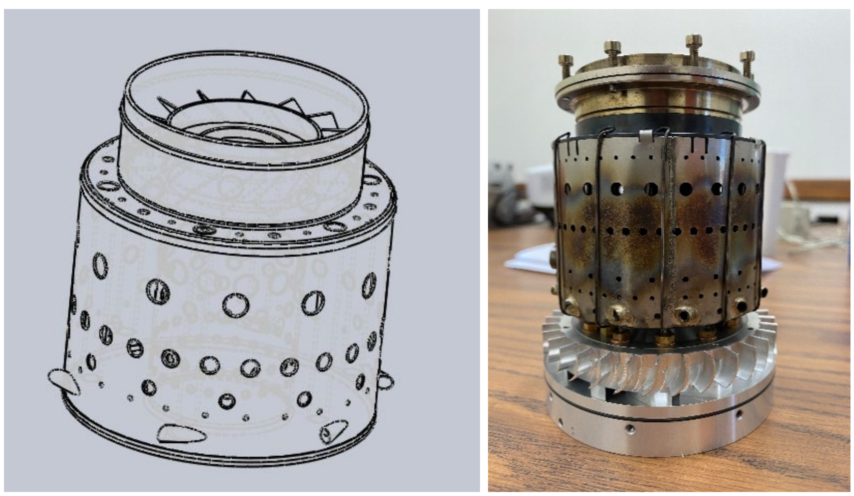

Figure 15. Combustion chamber model (left) and actual JetCat combustion chamber (right)

While the model is similar to the actual combustion chamber, there are a few differences to note. The first difference is the swirl inlets at the bottom of the chamber. The actual chamber has 12 swirl inlets, while the model only has 6. The other main difference is the fuel mixing tubes within the combustion chamber. The model has 6 tubes which run vertical within the chamber. The real JetCat has 12 tubes which run diagonal down the chamber, creating even more mixture in the reaction. These tubes were removed from the

CFX modeling. The high ignition temperatures of hydrogen could potentially melt these tubes in a real combustion process. This temperature would cause the metal to melt become FOD.

The combustion chamber cover was created in SolidWorks to create the fluid domain required for CFX. Once the cover was properly aligned to the combustion chamber, a fuel tube was inserted at the top and the combustion chamber was cut to a 60° slice to reduce the mesh size. The simulated fuel tube represents the actual fuel tube which wraps around the outside of the combustion chamber and enters through the fuel mixing tubes closest to the turbine side. The fuel mixing tubes were removed for the simulation because of hydrogens ability to combust faster than typical hydrocarbon fuels. The CFX geometry was generated by importing the geometry shown in Figure 16 and slicing the part with the combustion chamber model. The resulting geometry is shown in Figure 17.

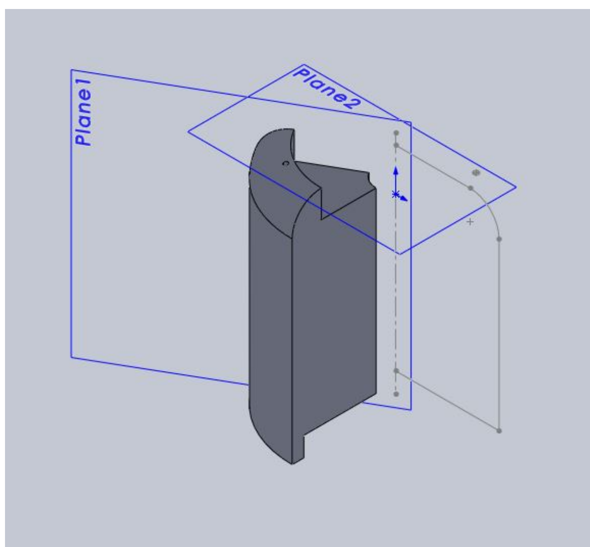

Figure 16. 60° combustion chamber cover with fuel inlet

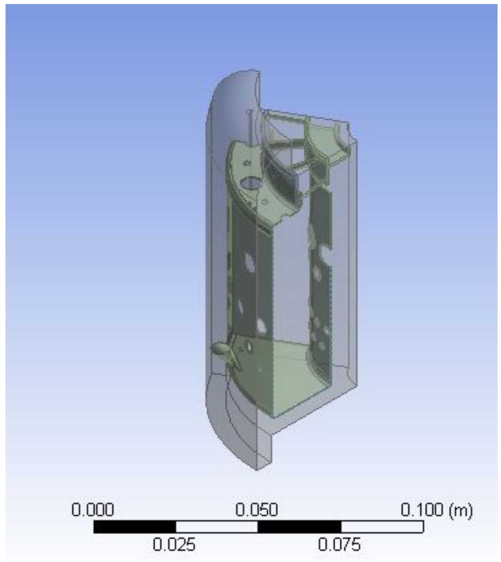

Figure 17. Sliced geometry used in CFX analysis

Once the combined geometry shown in Figure 17 was properly generated, a mesh was formed as shown in Figure 18. The mesh used the default conditions placed by CFX and did not include any additional methods or sizing factors to limit the already large computational mesh to reduce the computational load. The mesh contained 644,494 nodes and 3,417,235 elements. A new cylindrical coordinate system was generated to allow for a more accurate measuring system in CFX post.

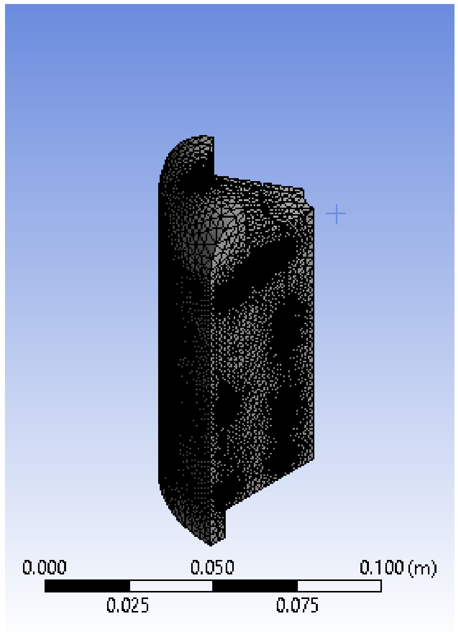

Figure 18. Mesh generated in CFX analysis

B. SETUP

The setup was modeled following the steps outlined in the ANSYS tutorial 20, 'Combustion and Radiation in a Can Combustor,' [10]. A GASTURB simulation for a JetCat engine operated with hydrogen fuel was also conducted to specify boundary conditions for CFX. Appendix D contains this GASTURB simulation data for propane and hydrogen fuel.

Initially, a hydrogen air mixture was selected from a pre-generated list of CFX mixtures. This was required in order to establish the fluids for the boundary conditions. Figure 19 shows the locations of the inputted boundaries.

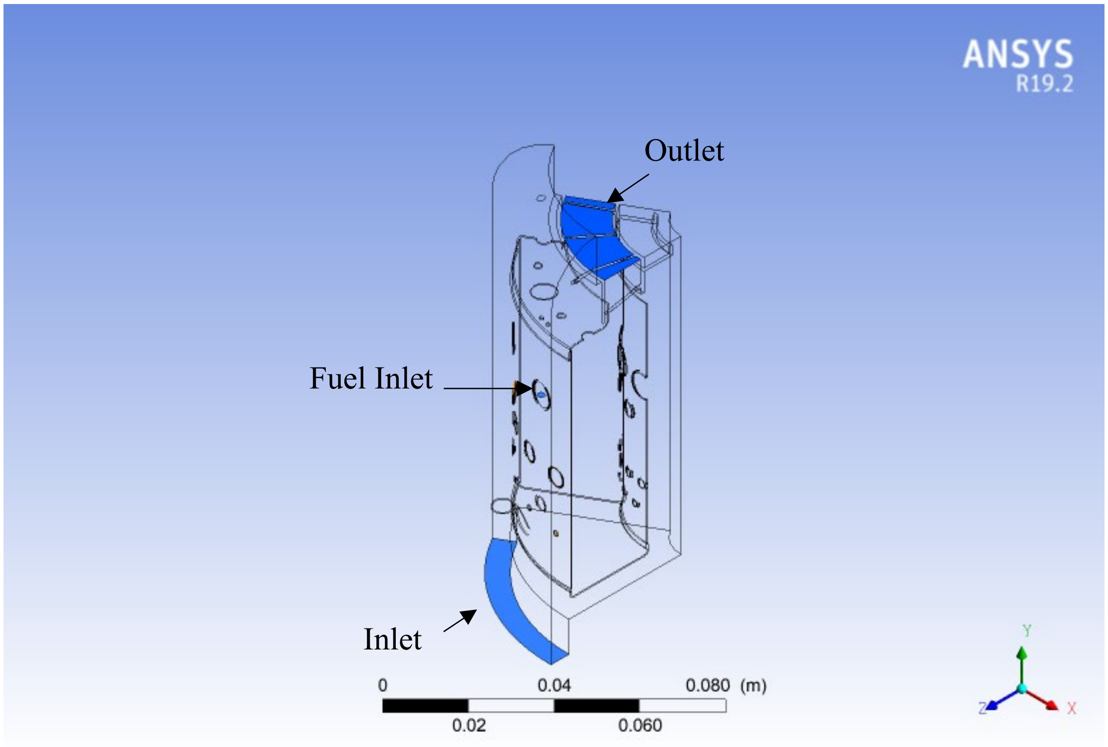

Figure 19. JetCat boundary locations

An additional domain interface with rotational periodicity was placed along the 60° cuts to simulate flow continuing throughout the combustion chamber. The specified boundary conditions can be found in Appendix E. The mass flow rates were calculated by dividing the GASTURB data of the entire engine by six to represent a 60° slice. The maximum adiabatic flame temperature of 2400 K was set to limit the maximum temperature of the simulation.

The globalization initial values are necessary to allow the simulation to have products of the reaction for the initial combustion to take place. The initial conditions for each component followed the tutorial except the component of CO2 was removed since no carbon is used in the reaction.

The solver control was set for upwind calculations. It was not adjusted to high resolution calculations because an error would occur after 1000 iterations when running with high resolution. The solution was steady state. The timescale control was set to auto timescale. The residual target was 1e-9. The solution was examined every 100 iterations to inspect the results. Once the combustion was sufficient, the data was analyzed.

C. HYDROGEN-AIR COMBUSTION RESULTS AND ANALYSIS

The solution was checked for convergence using the momentum and mass residuals. The momentum and mass residuals are shown in Figure 20. Appendix F contains the additional solution residuals.

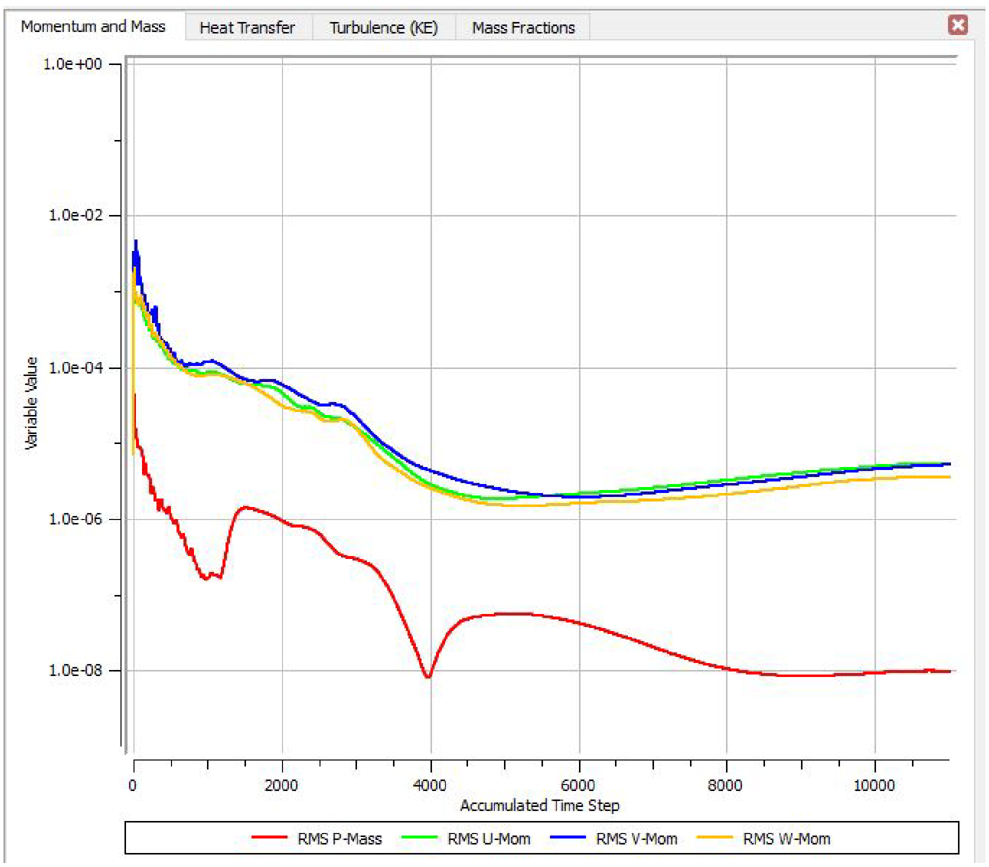

Figure 20. Momentum and mass residuals for hydrogen combustion CFX

Although it is not fully converged, the mass residuals are going slightly down and the momentum is slightly up. The flow is most likely unsteady but is being analyzed for a steady state solution. The solution stability was checked by calculating the heat addition.

The heat addition was calculated in CFX by subtracting the inlet and outlet enthalpies. The results were plotted at every 100 iterations throughout the entire solution and shown in Figure 21.

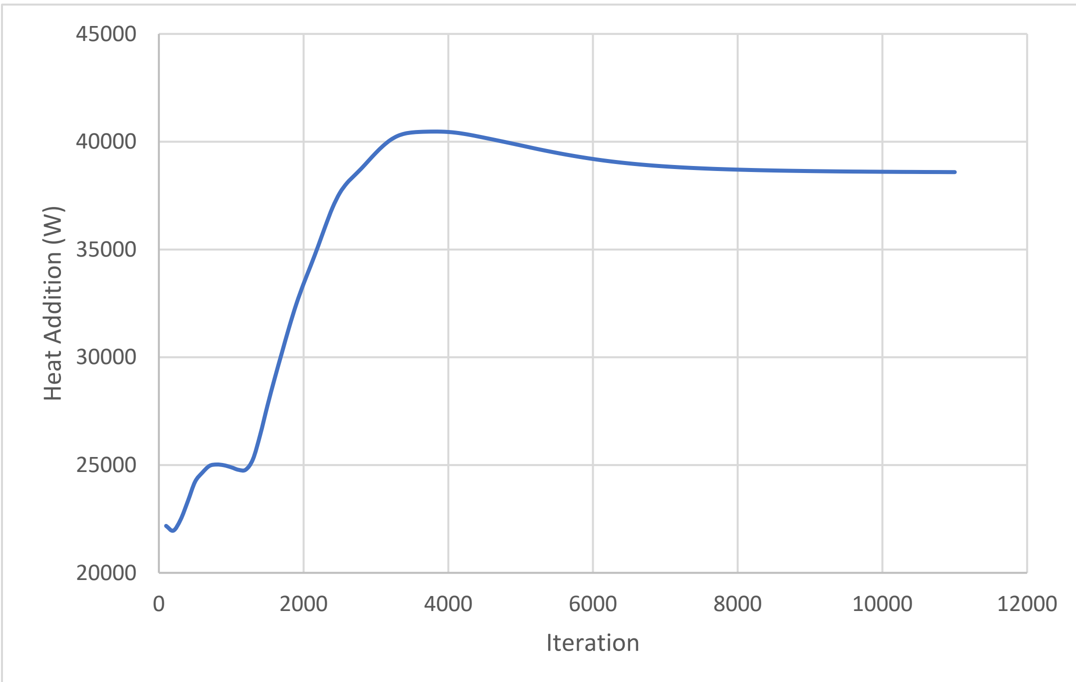

Figure 21. Heat addition throughout the combustion process

The heat addition in the combustion chamber starts off with a small increase until it drastically increases between 1200 to 3800 iterations. After it reaches a maximum heat addition of 40,470 W, the heat addition begins to level off with only a slight decrease after 8000 iterations. The simulation was run after 8000 iterations because the mass residuals were still increasing. Once the heat addition had consistently leveled off, the simulation was stopped.

Throughout the solution solver, the combustion chamber solution was observed every 100 iterations to capture the flame development. The flame development was analyzed to determine the high temperature regions of the liner and ensure the flame developed as expected for a hydrogen air mixture. Progressions of the flame development are shown in Figures 22, 23, 24, and 25.

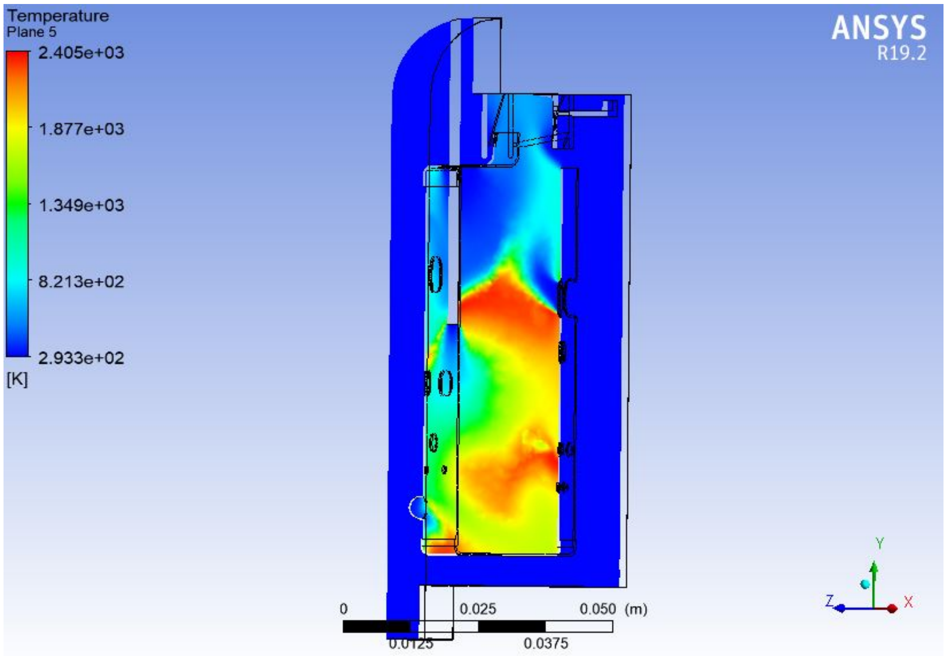

Figure 22. Hydrogen flame development at 1000 iterations

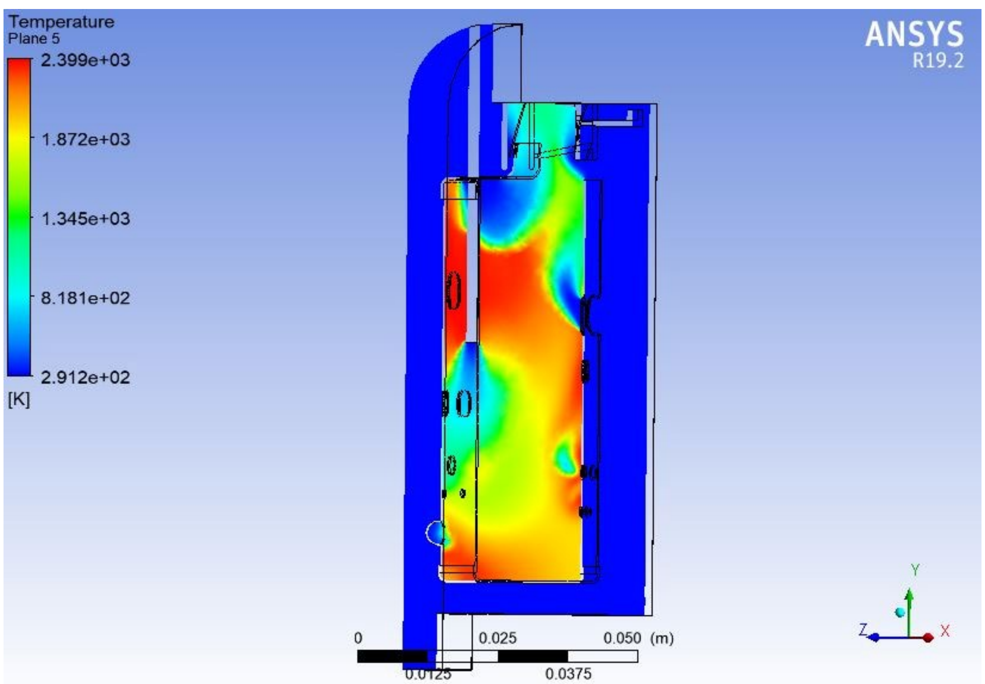

Figure 23. Hydrogen flame development at 3000 iterations

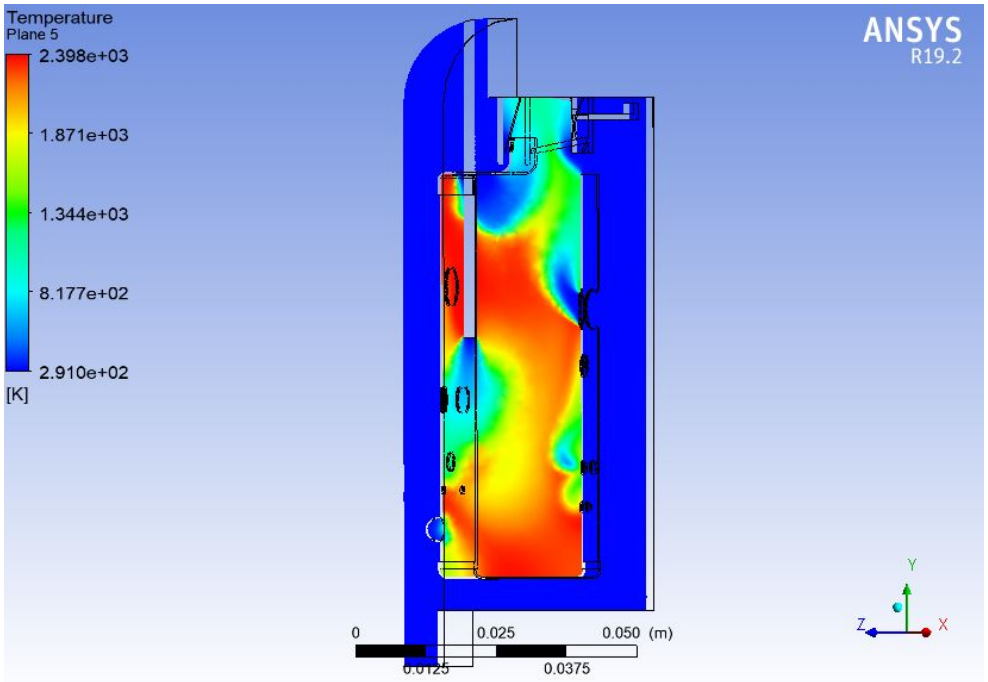

Figure 24. Hydrogen flame development at 7000 iterations

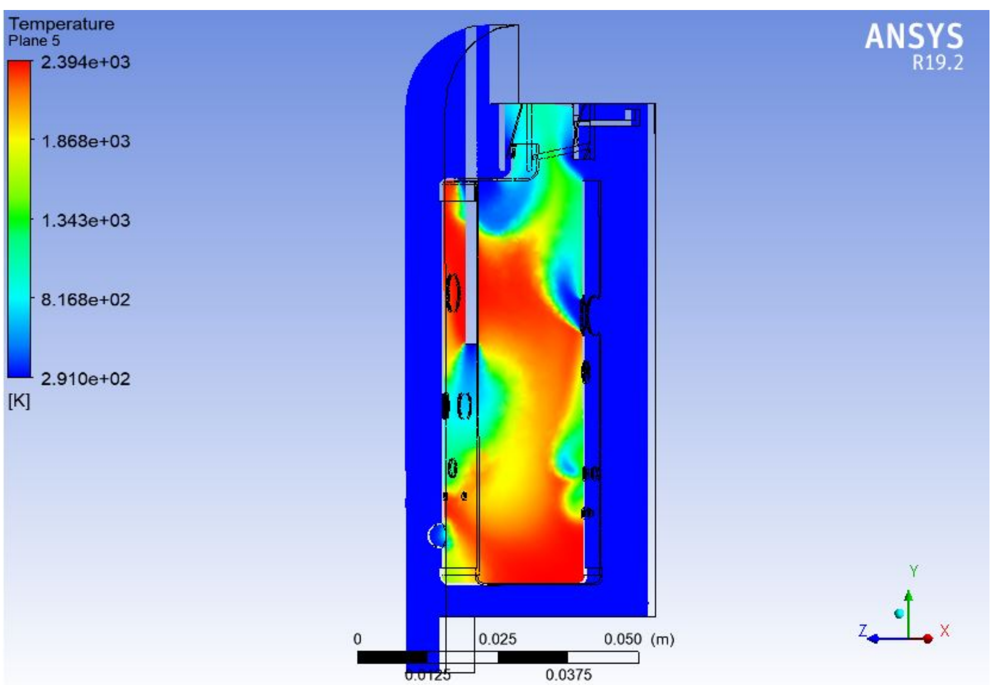

Figure 25. Hydrogen flame development at 11000 iterations

Initially, the flame is generated in the bottom of the combustion chamber. As the flame continues to develop, the hot air is pushed to the top of the chamber escapes through the outlet. The holes throughout the liner appear to be pushing cooler air through the chamber to focus the flame toward the middle of the chamber and away from the liner. Two large pockets of hot air are seen to form near the top and in the bottom inside of the combustion chamber. These two pockets contain air at 2400 K. This hot air has potential to melt through the combustion chamber liner depending on the material of the chamber. Redesign of the system may be required to lower the liner temperature.

The converged data was compared to the GASTURB data used to setup the CFX simulation. The two parameters compared were the combustion chamber exit temperature and combustion chamber pressure drop. The GASUTRB simulation calculated an exit temperature of 1080 K. The CFX simulation data was calculated by taking the area averaged temperature and pressure of the outlet. The average exit temperature was 915 K. The outlet area for 11000 iterations is shown in Figure 26.

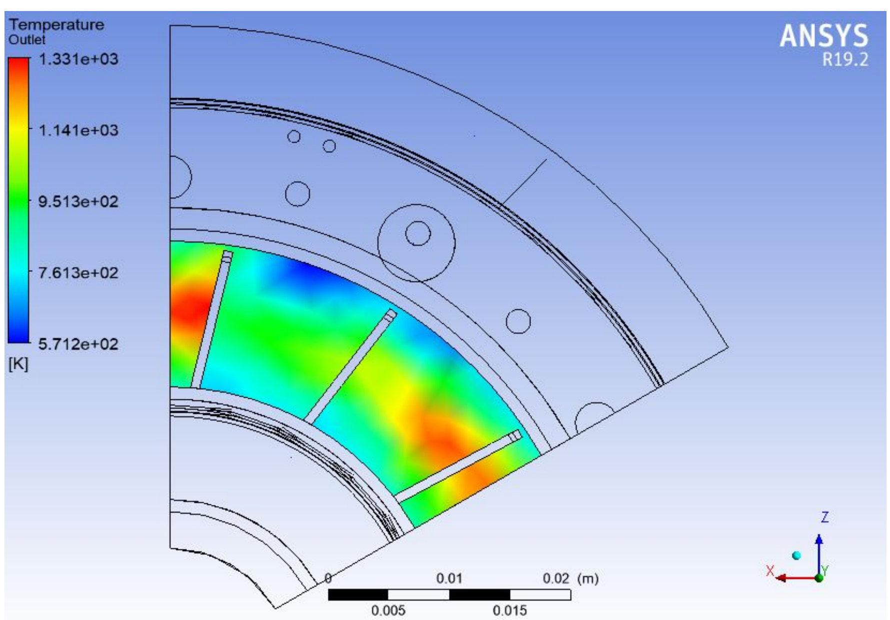

Figure 26. Combustion chamber outlet temperature at 11000 iterations

Lastly, the GASTURB simulation data between propane and hydrogen operations were compared against thrust specific fuel consumption (TSFC). The TSFC is important because it determines the weight of fuel needed for operation. The fuel comparison is shown in Table 5.

Table 5. Thrust specific fuel consumption for JetCat engine at max power

Thrust [kN]	0.06
Propane [g/(kN*s)]	42.0655
Hydrogen [g/(kN*s)]	15.1266

At identical power, hydrogen consumes almost three times less fuel by mass than propane. This difference allows hydrogen fueled gas turbine to have longer operational run times for the same mass in fuel.

D. DISCUSSION AND RECOMMENDATIONS

The JetCat combustion chamber simulations provided crucial data for future operation on hydrogen fuel. The data tells how the expected flame will form and flow, combustion chamber temperatures, and critical areas to analyze. The images of the flame shown in Figure 25 displays a high flame temperature at the top of the combustion chamber. One potential solution is to lower the fuel inlet location. Causing the tube to extend further down the combustion chamber can pull the flame closer to the center of the combustion chamber. It is important to ensure that the developed flame remains in the middle of the combustion chamber and does not exceed the melting point of the combustion chamber material. A centralized location will keep the high temperatures away from the compressor and turbine to minimize potential damages to crucial parts of the engine.

The outlet conditions help with verifying the GASTURB input data. Modification might need to be made to the GASTURB simulation to decrease combustion chamber exit temperature to match the simulation exit temperature. By manually lowering the exit temperature, compressor and turbine efficiencies will need to be adjusted to achieve the required 0.06 kN of thrust. This will also have an impact on the TSFC in Table 5.

The TSFC is an important parameter to because of its importance in increasing operational time using a hydrogen engine. This can have a major impact on DOD tactics and strategies if drones and other vehicles have longer operational times. Longer operational times can lead to fewer replenishments and refuelings.

To increase accuracy of results, a few additional changes should be made to the model. A mesh refinement study should occur to ensure the appropriately sized mesh is used. The solution solver should be adjusted from upwind to high resolutions. The CFX simulation should be setup to be a transient solver rather than a steady state solver. The fuel tube length should be varied to achieve the best heat affected zone (HAZ) for the combustion chamber. After these changes are implemented, new results can be compared to the GASTURB data prior to operational testing.

V. CONCLUSIONS AND FUTURE WORK

This thesis set out to achieve two primary goals: operate a gas turbine engine off hydrogen fuel and model a smaller JetCat engine for future experimental hydrogen runs. The C30 was able to successfully run with hydrogen fuel at different loads. The hydrogen results were compared to propane runs. Hydrogen fuel offers similar operating conditions and output power but only requires half the fuel by mass. The GASTURB simulations reinforce the experimental data and provide additional operating parameters.

The JetCat was able to be modeled and the simulation converged to a steady state solution for hydrogen fuel. The setup was aided by a GASTURB simulation which allowed for output parameters to be compared between the two simulations. Flame development images were collected to provide insight on modifications and potential hazards of hydrogen operation. TSFC was compared between propane and hydrogen fuel. It showed that hydrogen requires almost one-third the amount of fuel per mass than propane.

Hydrogen fuel has shown the ability to fulfill the desires and needs of the DOD and DON. Renewable energy can be used to generate and store hydrogen into high pressure tanks. Once fully compressed, hydrogen fuel has the ability to drastically increase operational time and decrease the need of refueling supply lines.

A. C30 CAPSTONE

The C30 Capstone should continue to be researched after a new hydrogen delivery system is installed. A larger delivery system will allow for more hydrogen to flow to the engine and allow the Capstone to operate at maximum power. Testing should be conducted at different pressure inputs and varying power loads. Future research could include a system design to incorporate hydrogen capture and compression with operation

B. JETCAT

The next stage of research for the JetCat should be to increase accuracy of the model. The flow should be simulated using a transient flow model with the following changes addressed: mesh refinement, solver solutions, and fuel tube length. The combustion chamber material should be checked for its ability to withstand the higher hydrogen flame temperature. Operational testing could then be conducted on the JetCat.

APPENDIX A. PROCEDURE FOR OPERATION WITH HYDROGEN

The procedure to run the C30 with hydrogen was created by Kaufmann [6]. The additional bold steps are included when running with the load bank and were generated as a part of this thesis.

1. Verify that there are no leaks and that no power is supplied to the solenoid valves.
2. **Connect the load bank's ground cam-lock to an earth ground [8].**
3. **Ensure all panel switches are in the off position [8].**
4. **Keep load bank clear so air will flow freely [8].**
5. **Connect power plug to the unit [8].**
6. **Connect cam-locks to the unit [8].**
7. **Turn the Main Power switch to the ON position and the Master Load switch OFF [8].**
8. Move the battery isolation switch to the ON position, accessible via the panel labeled "BATTERY CIRCUIT BREAKER ACCESS SWITCH" [11].
9. Press the "BATT START" button (accessible via the control panel, labeled with the Capstone logo) to wake the C30 from sleep mode [11].
10. Verify that the C30 is configured for Stand Alone Operation. If not already in Stand Alone Operation Mode, configure the C30 as described in Chapter 3 of reference [11] and in reference [12].
11. Start the CRMS software, previously installed on a laptop with a RS-232 serial port [13].
12. Connect the computer to the C30 and establish communications. Open the Communications Bay to access the User Connection Board and the User Port (J6) in accordance with section 2.1, User Interface [11]. Connect the computer' RS-232 serial port to the C30 RS-232 serial port using a null modem cable. Attempts to extend the cable by connecting it in series with another modem cable are not recommended.

13. Select the “Display” tab from the options bar in the “Unit_1” window. Select “Strip Chart.”
14. Once the chart labelled “Microturbine Chart, Unit_1” appears, select the desired parameters from the drop-down menus. No more than four parameters are recommended to avoid visual clutter unless specifically required for real-time observation. All parameters will have data collected and may be charted/graphed later. The recommended parameters are “Turbine Exit Temperature,” “Battery SOC,” “Compressor Inlet Temperature,” and “Engine Speed” for a no-load run. Adjust the number of points to cover the expected runtime of the turbine. Beneath each parameter, select the upper and lower bounds. The y-axis ranges from 0 to 1, with each parameter being charted as a decimal percentage of its upper bound [13]. Recommend zero to above maximum value achieved. Avoid setting expected values such that multiple parameters chart at similar values (i.e., 0.8 for both TET and Bat SOC).
15. Select “Control Mode” from the mode drop-down menu. If prompted for a password, enter the default user port user password <USR123P> or the selected user port user password [13].
16. Select the save “File Manager” button in the top ribbon. The toggle button “Recording” should be set to manual within the “Data Recording” pane. Click the radio button “Start Recording” within the same pane; when it appears green and says “ON,” close the window. The file location may also be changed to user preference.
17. Manually open the H_2 tank valve and the manual shutoff valve.
18. Adjust the regulator to the desired fuel supply pressure.
19. Evacuate the area. (One of the test cells at the TPL was used to provide a safe barrier between the C30 and the user in the event of uncontrolled combustion.)
20. Open solenoid valve 1 remotely.
21. Open solenoid valve 2 remotely and vent for 2–4 seconds to flush the supply system with H_2 and reduce the chance of flashback.
22. Close solenoid valve 2 remotely.

23. Click “START” under “Turbine Start” and allow the C30 to start up and run [13].
24. **Place the desired test step switch in the ON [8].**
25. **Place the Master Load switch in the ON to engage the resistors [8].**
26. Observe data collection/conduct experiment.
27. Click “STOP” under “Turbine Start” and allow the C30 to run its shutdown procedure. In the event of an automatic shutdown and an error message, allow the C30 to safely stop on its own [13].
28. Verify that the C30 has stopped.
29. **Place all switches in the OFF position. Place Master Load in the OFF position [8].**
30. **Allow fans to operate at least three minutes or until exhaust air is cool before shutting them off [8].**
31. **Turn Main Power Switch to the OFF position and remove control power [8].**
32. Close solenoid valve 1 remotely.
33. Vent the remaining H_2 in the supply line by actuating solenoid valve 2 remotely.
34. Close the manual shutoff valve and the H_2 tank valve.
35. Turn off the control panel by moving the battery isolation switch into the OFF position, accessible via the panel labeled “BATTERY CIRCUIT BREAKER ACCESS SWITCH” [11].
36. Save the collected data and disconnect the computer from the C30.

THIS PAGE INTENTIONALLY LEFT BLANK

APPENDIX B. C30 GASTURB INPUTS AND OUTPUTS

A. PROPANE INPUTS

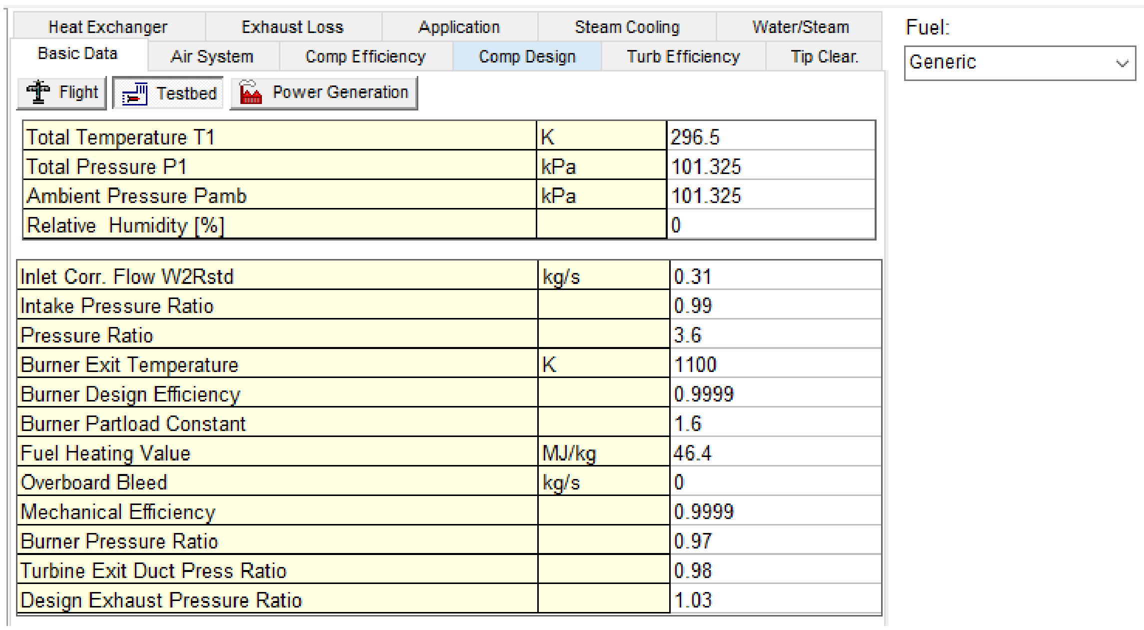

Total Temperature T1	K	296.5
Total Pressure P1	kPa	101.325
Ambient Pressure Pamb	kPa	101.325
Relative Humidity [%]		0

Inlet Corr. Flow W2Rstd	kg/s	0.31
Intake Pressure Ratio		0.99
Pressure Ratio		3.6
Burner Exit Temperature	K	1100
Burner Design Efficiency		0.9999
Burner Partload Constant		1.6
Fuel Heating Value	MJ/kg	46.4
Overboard Bleed	kg/s	0
Mechanical Efficiency		0.9999
Burner Pressure Ratio		0.97
Turbine Exit Duct Press Ratio		0.98
Design Exhaust Pressure Ratio		1.03

Figure 27. C30 basic data inputs (generic/propane)

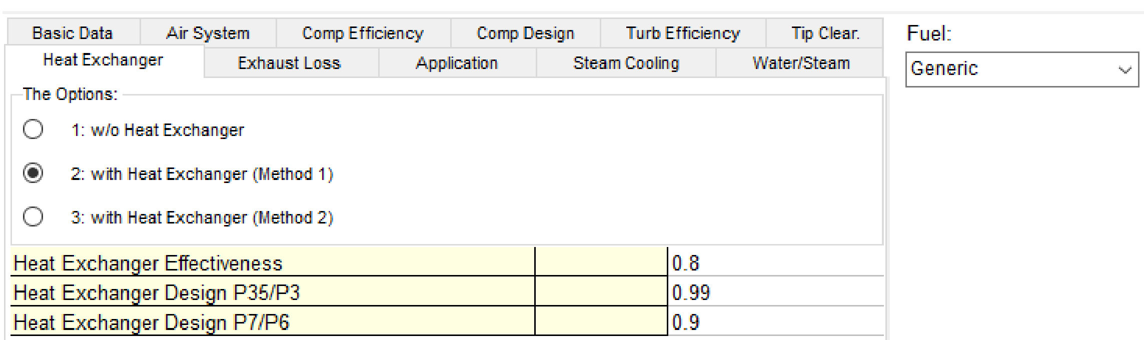

Heat Exchanger Effectiveness		0.8
Heat Exchanger Design P35/P3		0.99
Heat Exchanger Design P7/P6		0.9

Figure 28. C30 heat exchanger data inputs (generic/propane)

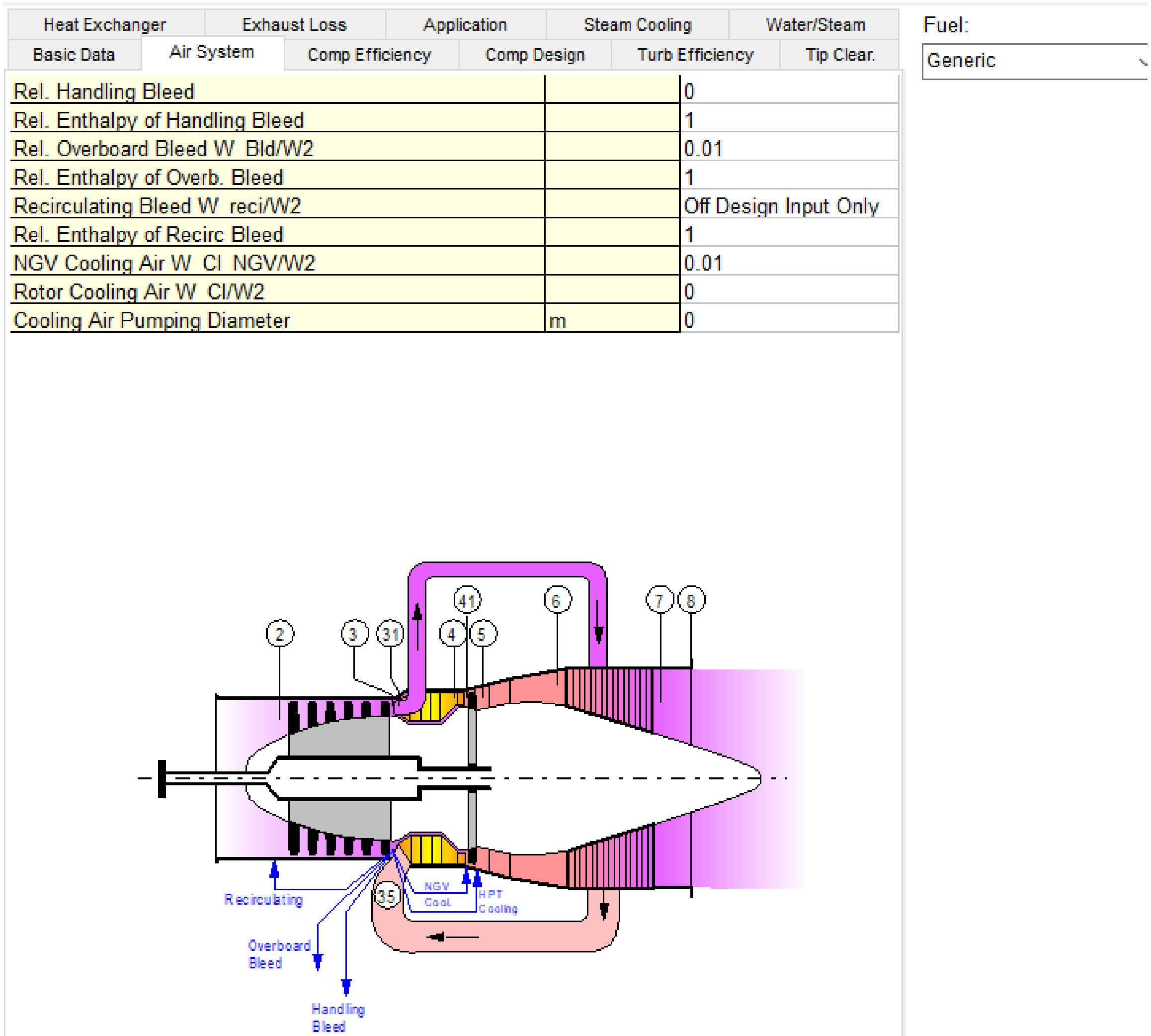

Figure 29. C30 air system data inputs (generic/propane)

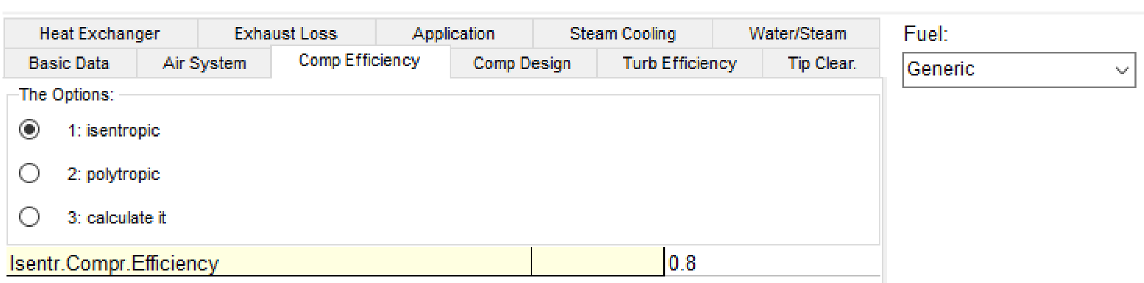

Figure 30. C30 compressor efficiency data inputs (generic/propane)

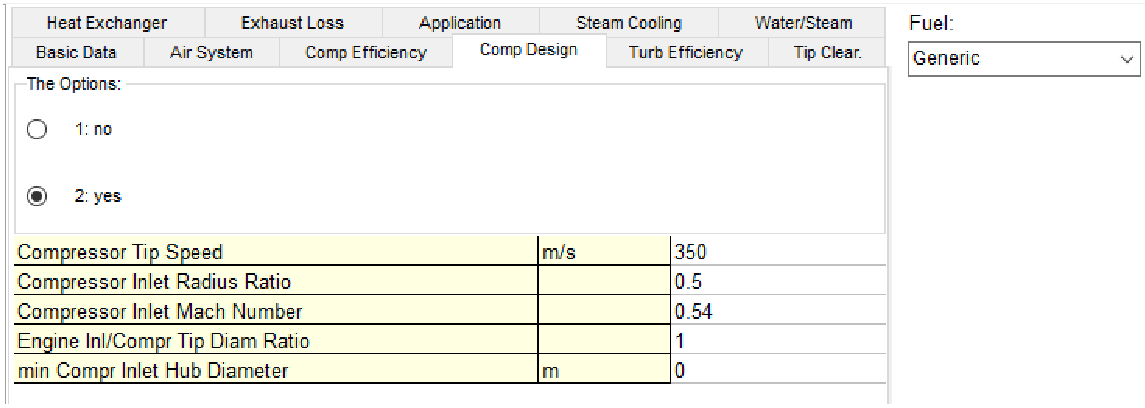

Figure 31. C30 compressor design data inputs (generic/propane)

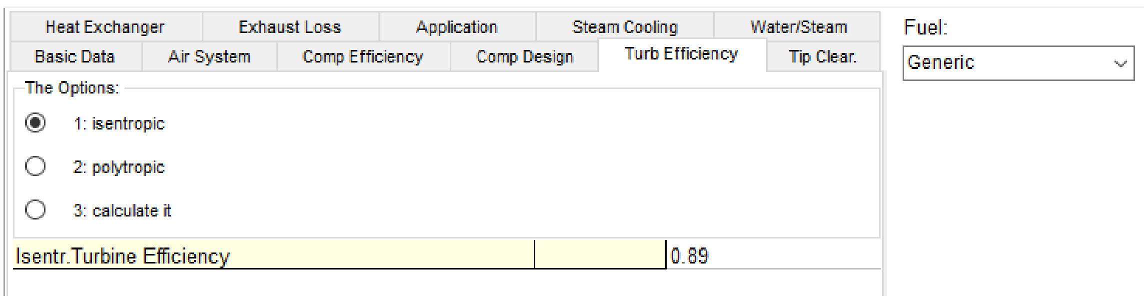

Figure 32. C30 turbine efficiency data inputs (generic/propane)

B. PROPANE OUTPUTS

```
Summary | Compressor | Air System

          W          T          P          WRstd
Station   kg/s       K          kPa        kg/s       PWSD      =       30.1 kW
 amb                 296.50     101.325
  1       0.303      296.50     101.325               PSFC      =     0.3048 kg/(kW*h)
  2       0.303      296.50     100.312    0.310      Heat Rate=   13143.5 kJ/(kW*h)
  3       0.303      458.91     361.122    0.107      Therm Eff=     0.2739
 31       0.300      458.91     361.122               WF        =   0.00255 kg/s
 35       0.296      786.65     357.511               P35/P3    =   0.99000
  4       0.299     1100.00     346.786    0.171      P7/P6     =   0.90000
 41       0.302     1096.96     346.786    0.172      s NOx     =   0.39390
 49       0.302      867.20     118.327               incidence=    0.00000 °
  5       0.302      867.20     118.327    0.449      XM8       =     0.2077
  6       0.302      867.20     115.961               A8        =     0.0049 m²
  7       0.302      551.97     104.365
  8       0.302      551.97     104.365    0.406      P8/Ps8    =   1.03000
Bleed     0.003      458.91     361.122               WBld/W2   =   0.01000
---------------------------------------------         P2/P1     =   0.99000
Efficiencies:    isentr  polytr    RNI    P/P         W_NGV/W2  =   0.01000
 Compressor      0.8000  0.8318  0.957  3.600         WCL/W2    =   0.00000
 Burner          0.9999                 0.970         Loading   =    100.00 %
 Turbine         0.8900  0.8757  0.712  2.931         e45 th    =   0.88988
 Heat Exch.      0.8000
 Generator       1.0000                               PW_gen    =       30.1 kW
---------------------------------------------
Spool mech Eff   0.9999  Nom Spd   126984 rpm         P6/P5     =     0.9800
---------------------------------------------

hum [%]     war0        FHV      Fuel
   0.0    0.00000     43.124     Generic
```

Figure 33. C30 summary of outputs (generic/propane)

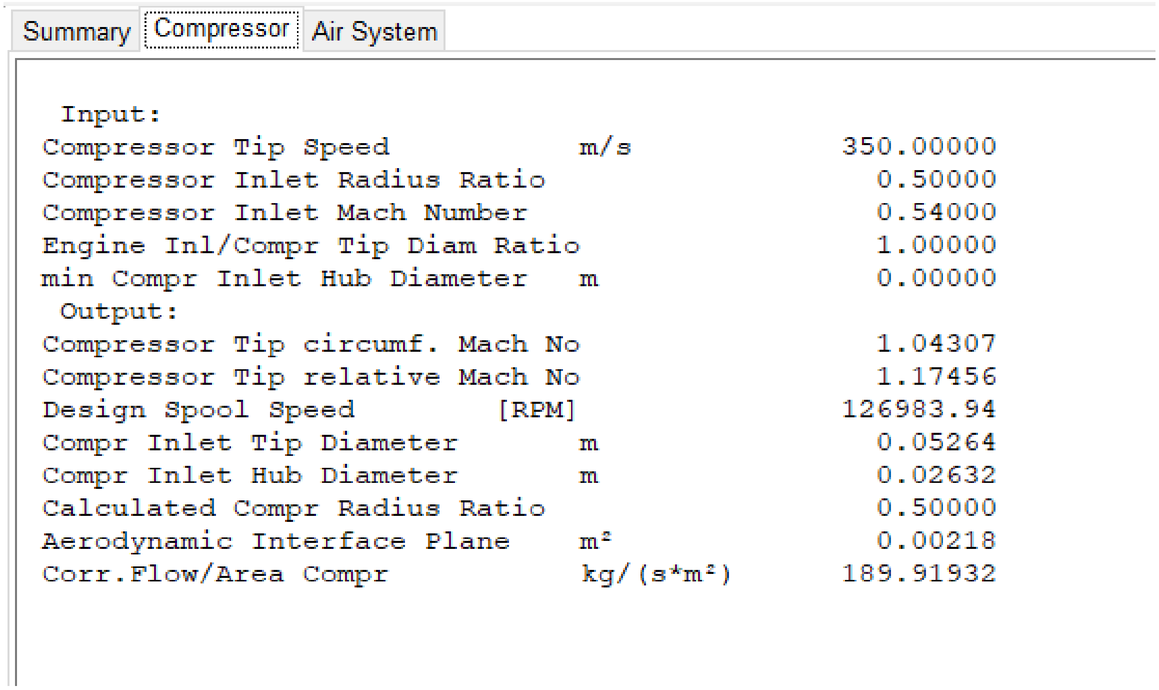

Summary | Compressor | Air System

Input:		
Compressor Tip Speed	m/s	350.00000
Compressor Inlet Radius Ratio		0.50000
Compressor Inlet Mach Number		0.54000
Engine Inl/Compr Tip Diam Ratio		1.00000
min Compr Inlet Hub Diameter	m	0.00000
Output:		
Compressor Tip circumf. Mach No		1.04307
Compressor Tip relative Mach No		1.17456
Design Spool Speed	[RPM]	126983.94
Compr Inlet Tip Diameter	m	0.05264
Compr Inlet Hub Diameter	m	0.02632
Calculated Compr Radius Ratio		0.50000
Aerodynamic Interface Plane	m²	0.00218
Corr.Flow/Area Compr	kg/(s*m²)	189.91932

Figure 34. C30 compressor data outputs (generic/propane)

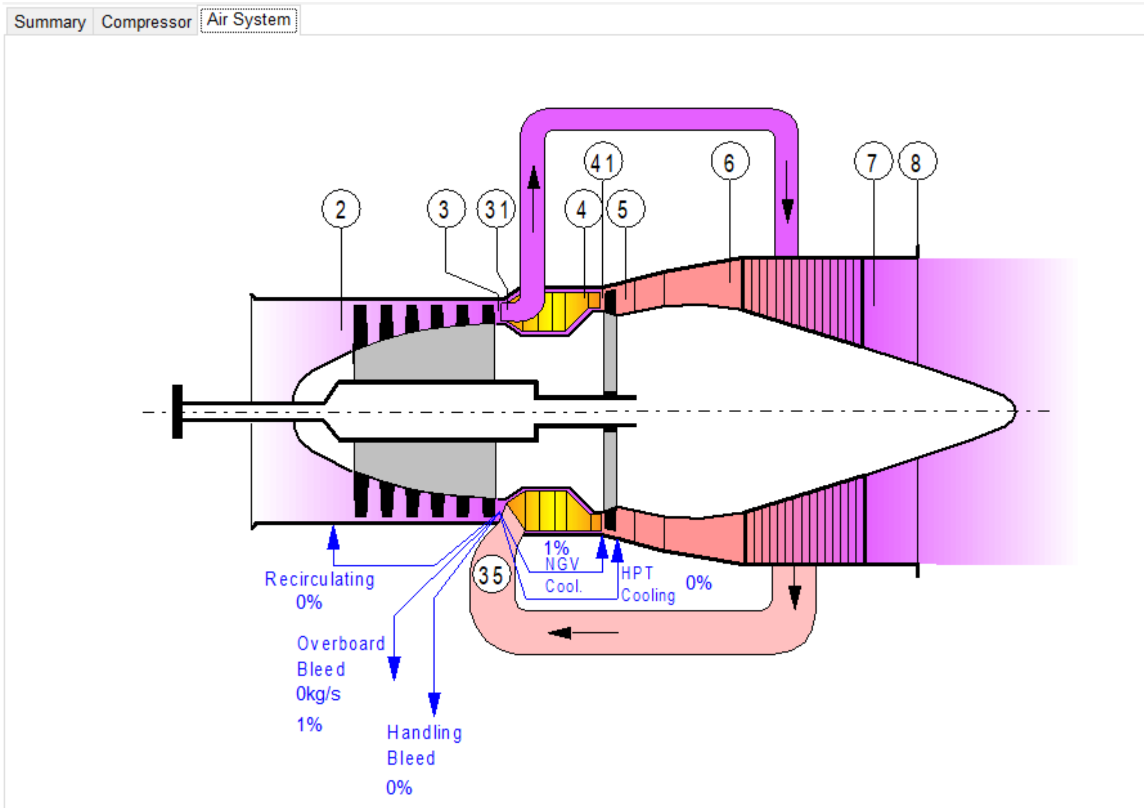

Figure 35. C30 air system outputs (generic/propane)

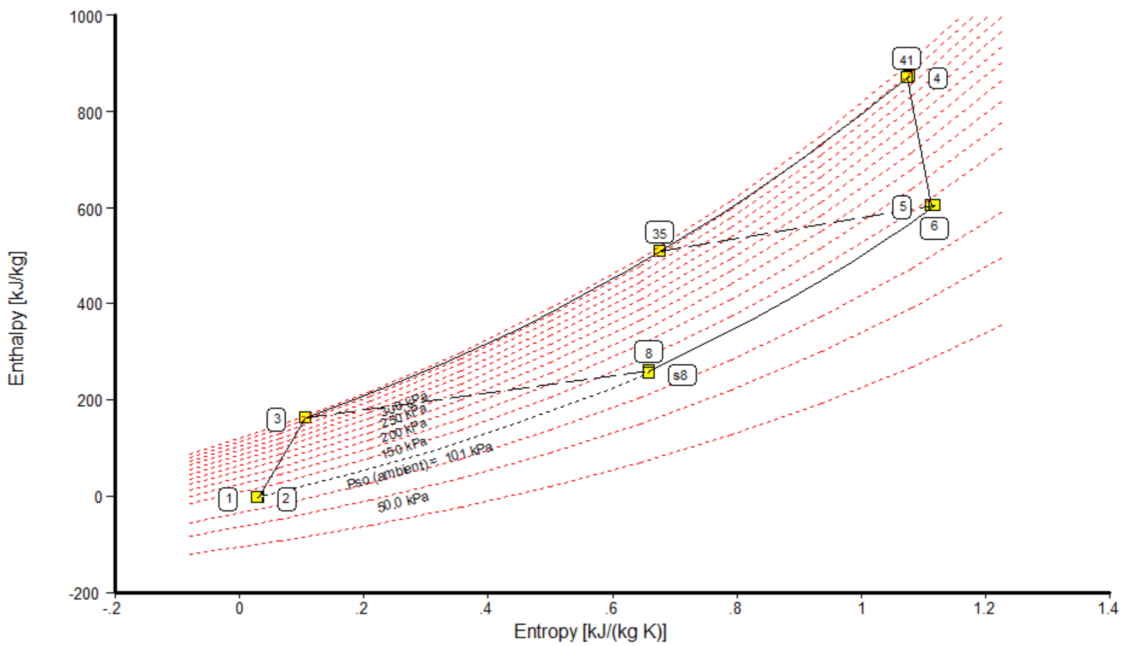

Figure 36. C30 enthalpy-entropy diagram (generic/propane)

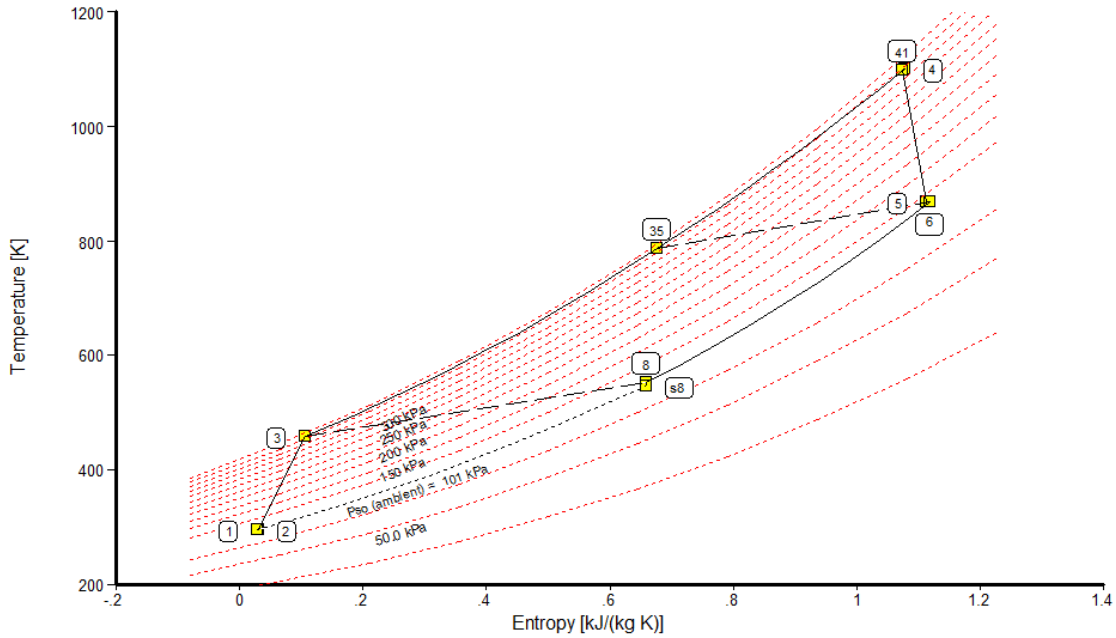

Figure 37. C30 temperature-entropy diagram(generic/propane)

C. HYDROGEN INPUTS

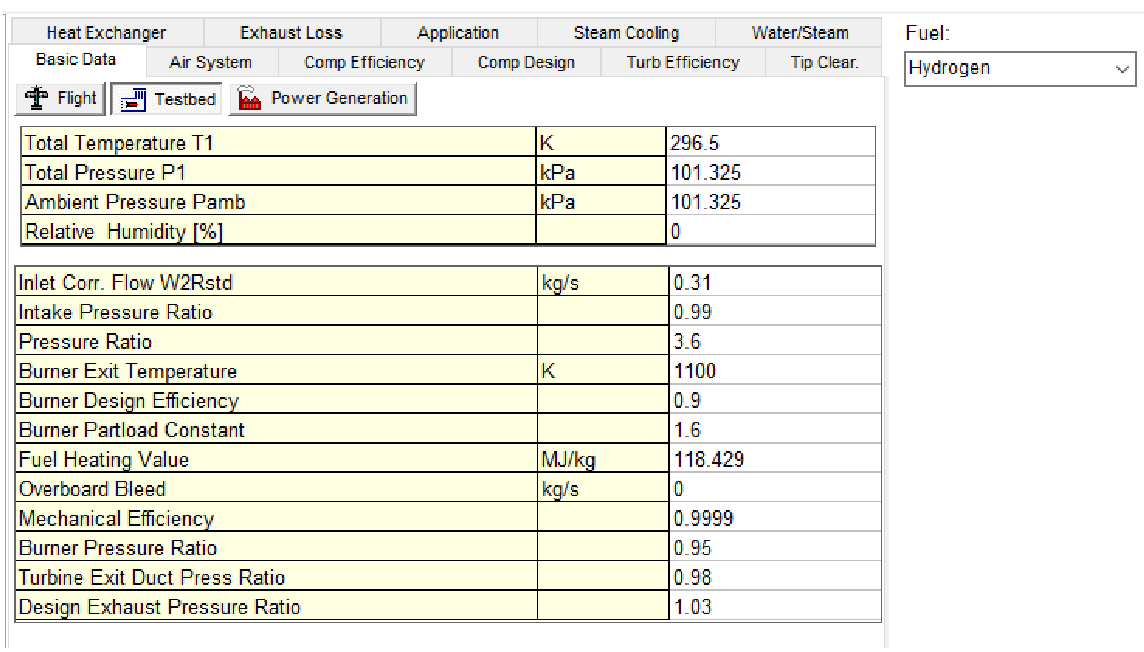

Total Temperature T1	K	296.5
Total Pressure P1	kPa	101.325
Ambient Pressure Pamb	kPa	101.325
Relative Humidity [%]		0

Inlet Corr. Flow W2Rstd	kg/s	0.31
Intake Pressure Ratio		0.99
Pressure Ratio		3.6
Burner Exit Temperature	K	1100
Burner Design Efficiency		0.9
Burner Partload Constant		1.6
Fuel Heating Value	MJ/kg	118.429
Overboard Bleed	kg/s	0
Mechanical Efficiency		0.9999
Burner Pressure Ratio		0.95
Turbine Exit Duct Press Ratio		0.98
Design Exhaust Pressure Ratio		1.03

Figure 38. C30 basic data inputs (hydrogen)

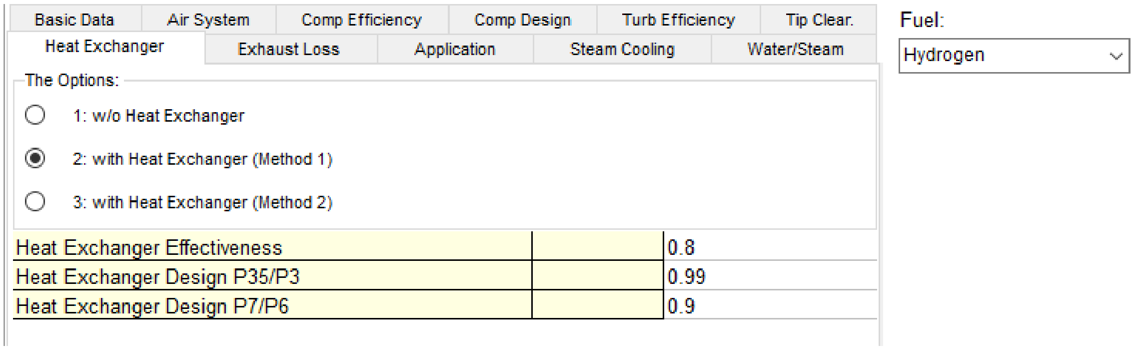

Figure 39. C30 heat exchanger inputs (hydrogen)

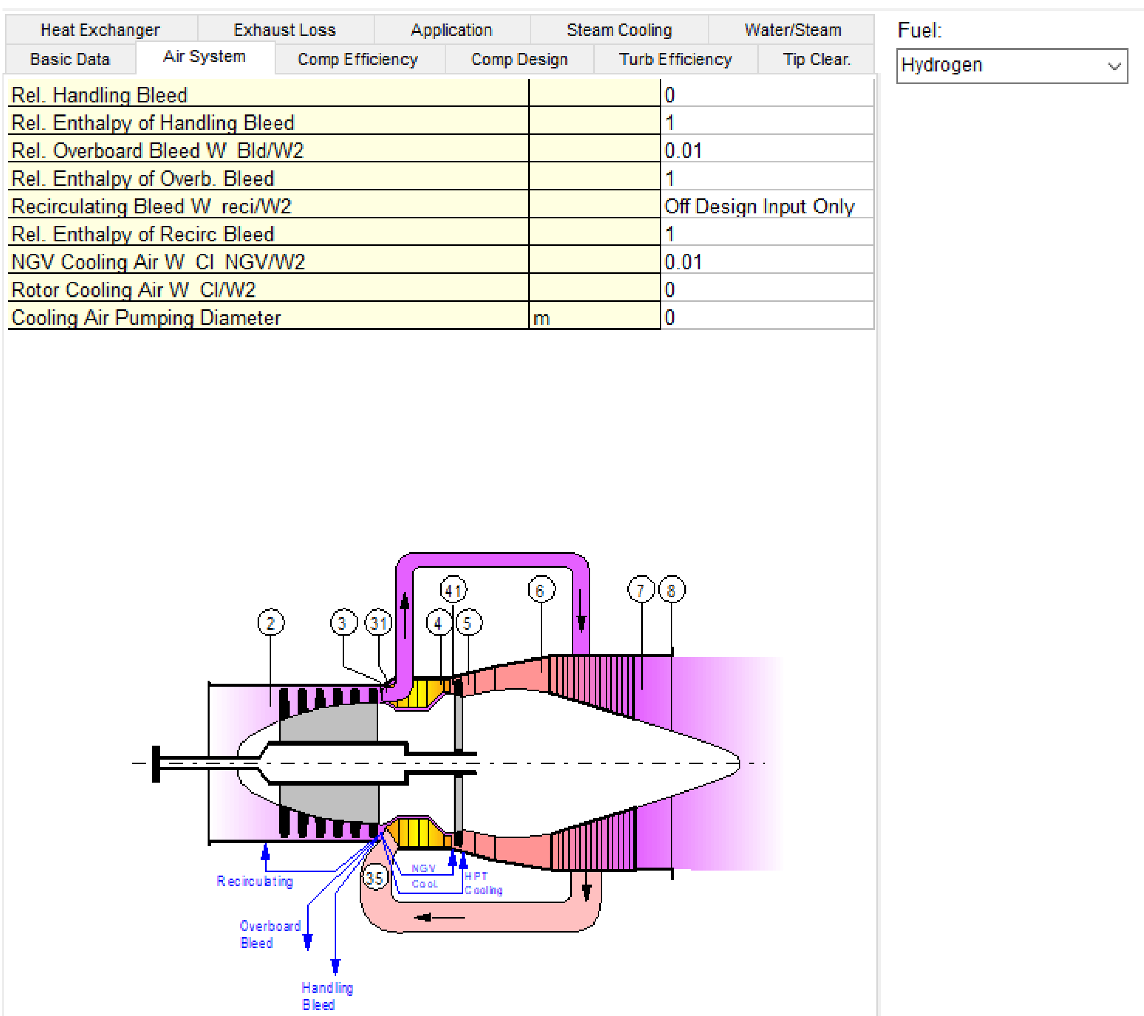

Figure 40. C30 air system inputs (hydrogen)

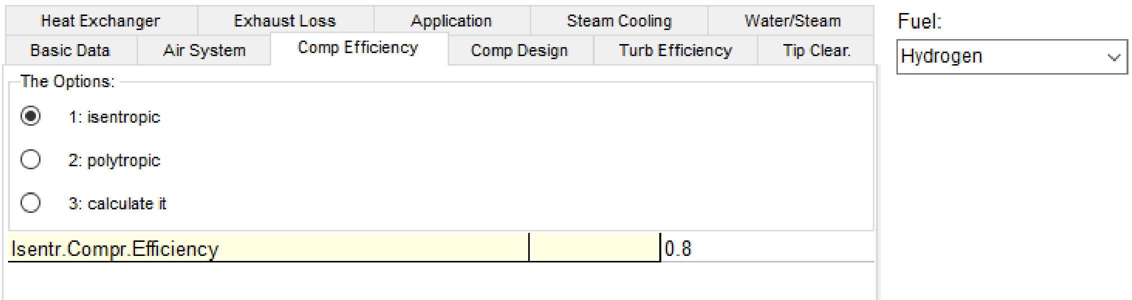

Figure 41. C30 compressor efficiency inputs (hydrogen)

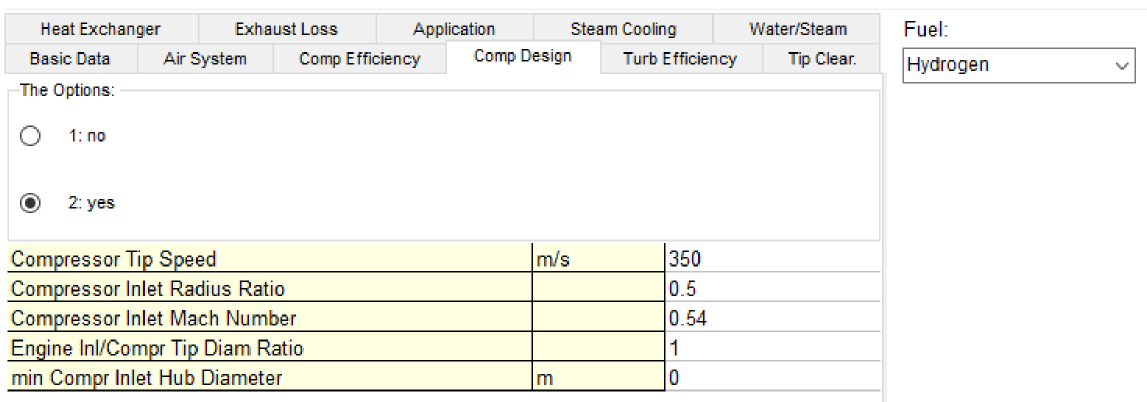

Figure 42. C30 compressor design inputs (hydrogen)

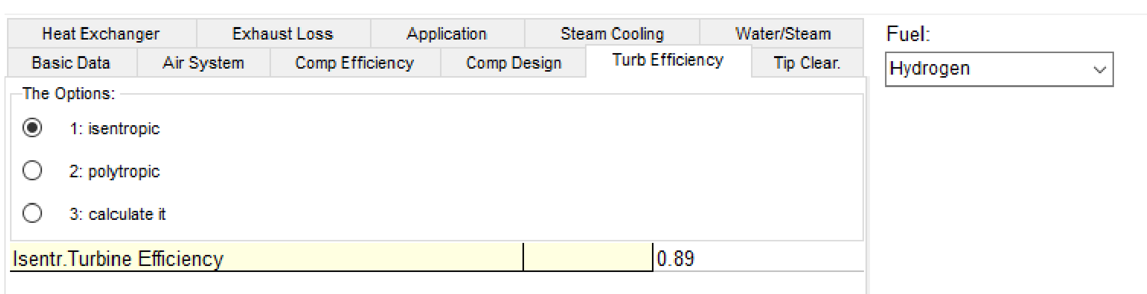

Figure 43. C30 turbine efficiency inputs (hydrogen)

D. HYDROGEN OUTPUTS

```
Summary | Compressor | Air System

          W          T          P          WRstd
Station   kg/s       K          kPa        kg/s        PWSD      =      30.1 kW
 amb                 296.50     101.325
  1       0.303      296.50     101.325                PSFC      =    0.1242 kg/(kW*h)
  2       0.303      296.50     100.312    0.310       Heat Rate=   14709.7 kJ/(kW*h)
  3       0.303      458.90     361.122    0.107       Therm Eff=    0.2447
 31       0.300      458.90     361.122                WF        =   0.00104 kg/s
 35       0.296      789.40     357.511                P35/P3    =   0.99000
  4       0.298     1100.00     339.636    0.175       P7/P6     =   0.90000
 41       0.301     1097.03     339.636    0.177       s NOx     =   0.39951
 49       0.301      870.50     118.327                incidence=   0.00000 °
  5       0.301      870.50     118.327    0.452       XM8       =    0.2079
  6       0.301      870.50     115.961                A8        =    0.0049 m²
  7       0.301      556.80     104.365
  8       0.301      556.80     104.365    0.409       P8/Ps8    =   1.03000
Bleed     0.003      458.90     361.122                WBld/W2   =   0.01000
--------------------------------------------           P2/P1     =   0.99000
Efficiencies:    isentr  polytr    RNI    P/P          W_NGV/W2  =   0.01000
 Compressor      0.8000  0.8318   0.957  3.600         WCL/W2    =   0.00000
 Burner          0.9000                  0.950         Loading   =    100.00 %
 Turbine         0.8900  0.8760   0.697  2.870         e45 th    =   0.88976
 Heat Exch.      0.8000
 Generator       1.0000                                PW_gen    =      30.1 kW
--------------------------------------------
Spool mech Eff   0.9999  Nom Spd   126984 rpm          P6/P5     =    0.9800
--------------------------------------------

hum [%]     war0       FHV      Fuel
   0.0   0.00000   118.429    Hydrogen
```

Figure 44. C30 summary of outputs (hydrogen)

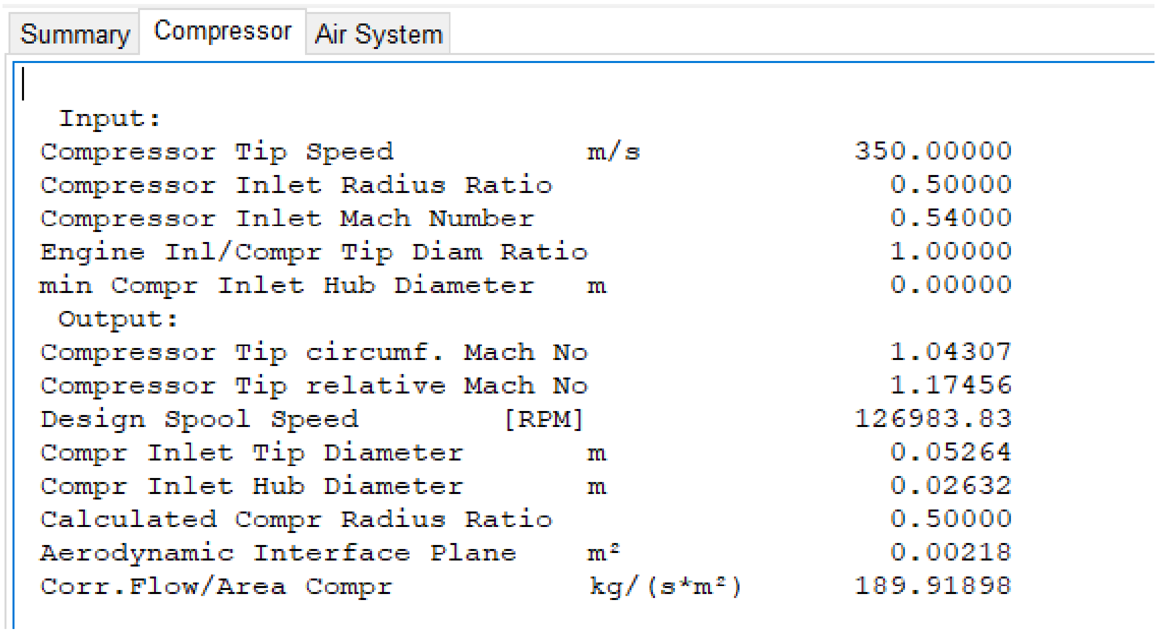

Summary | Compressor | Air System

Input:

Compressor Tip Speed	m/s	350.00000
Compressor Inlet Radius Ratio		0.50000
Compressor Inlet Mach Number		0.54000
Engine Inl/Compr Tip Diam Ratio		1.00000
min Compr Inlet Hub Diameter	m	0.00000

Output:

Compressor Tip circumf. Mach No		1.04307
Compressor Tip relative Mach No		1.17456
Design Spool Speed	[RPM]	126983.83
Compr Inlet Tip Diameter	m	0.05264
Compr Inlet Hub Diameter	m	0.02632
Calculated Compr Radius Ratio		0.50000
Aerodynamic Interface Plane	m^2	0.00218
Corr.Flow/Area Compr	$kg/(s*m^2)$	189.91898

Figure 45. C30 compressor data outputs (hydrogen)

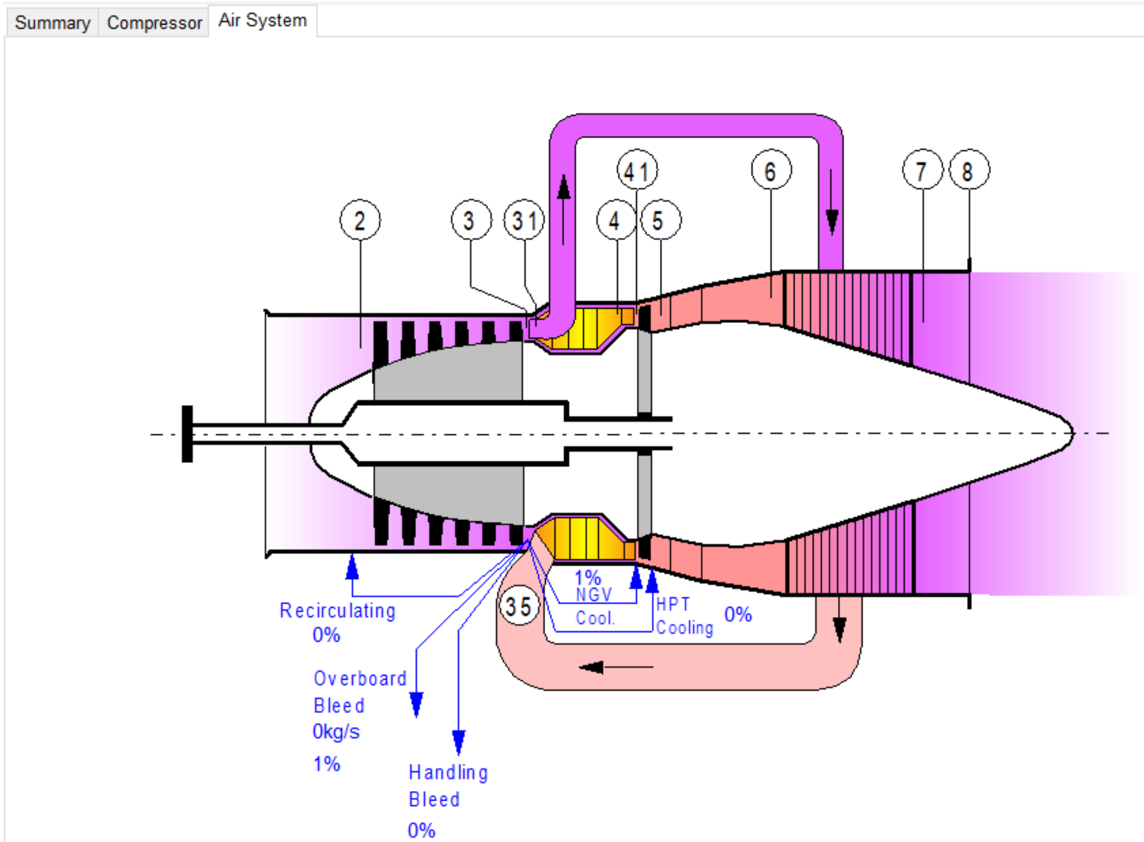

Figure 46. C30 air system outputs (hydrogen)

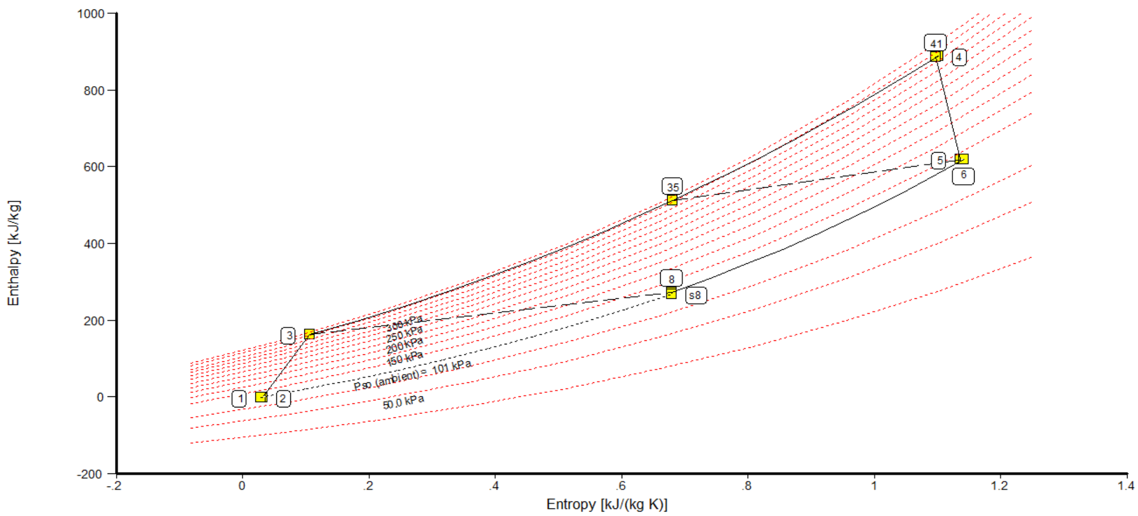

Figure 47. C30 enthalpy-entropy diagram (hydrogen)

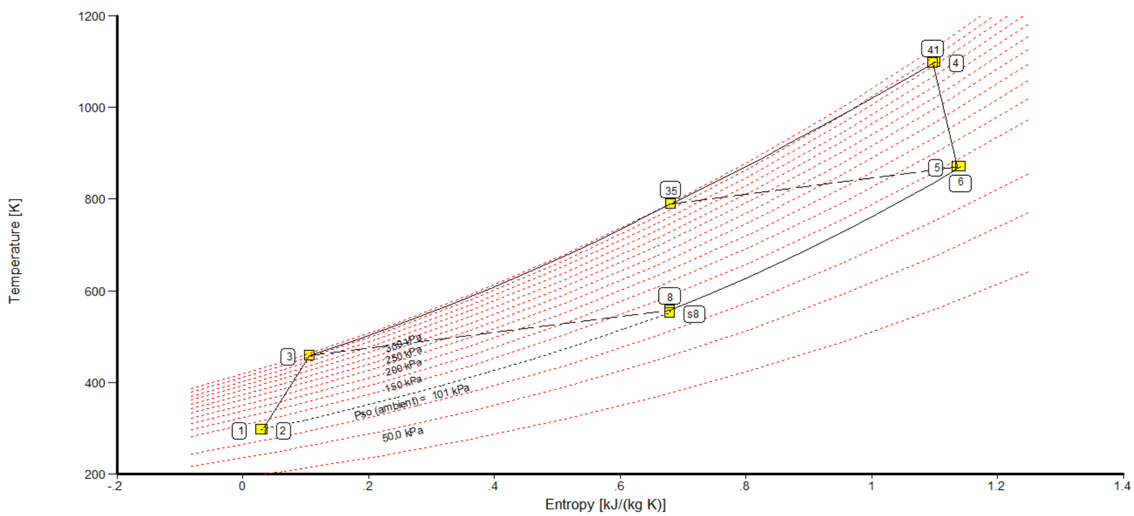

Figure 48. C30 temperature-entropy diagram (hydrogen)

APPENDIX C. C30 HYDROGEN FUEL MASS FLOW CALCULATIONS

Using the hydrogen 6 pack pressure readings and the ideal gas law, the mass flow of hydrogen fuel was able to be calculated. Because of the phase change occurring in propane fuel, only hydrogen mass flow was calculated. The temperature was assumed to be at standard conditions.

$$pV = mRT$$

$$m = \frac{pV}{RT}$$

$$\dot{m} = \frac{m}{s}, \text{ s is run time in seconds}$$

Load (kW)	Starting Pressure (kPa)	Ending Pressure (kPa)	Run time (s)
15	11721	11376	90
20	11376	10895	90

Load (kW)	Mass Beginning (kg)	Mass End (kg)	Mass difference (kg)	Mass Flow (kg/s)
15	2.4590	2.3866	0.0724	8.04E-04
20	2.3866	2.2857	0.1009	1.12E-03

THIS PAGE IS INTENTIALLY LEFT BLANK

APPENDIX D. JETCAT GASTURB INPUTS AND OUTPUTS

A. PROPANE INPUTS

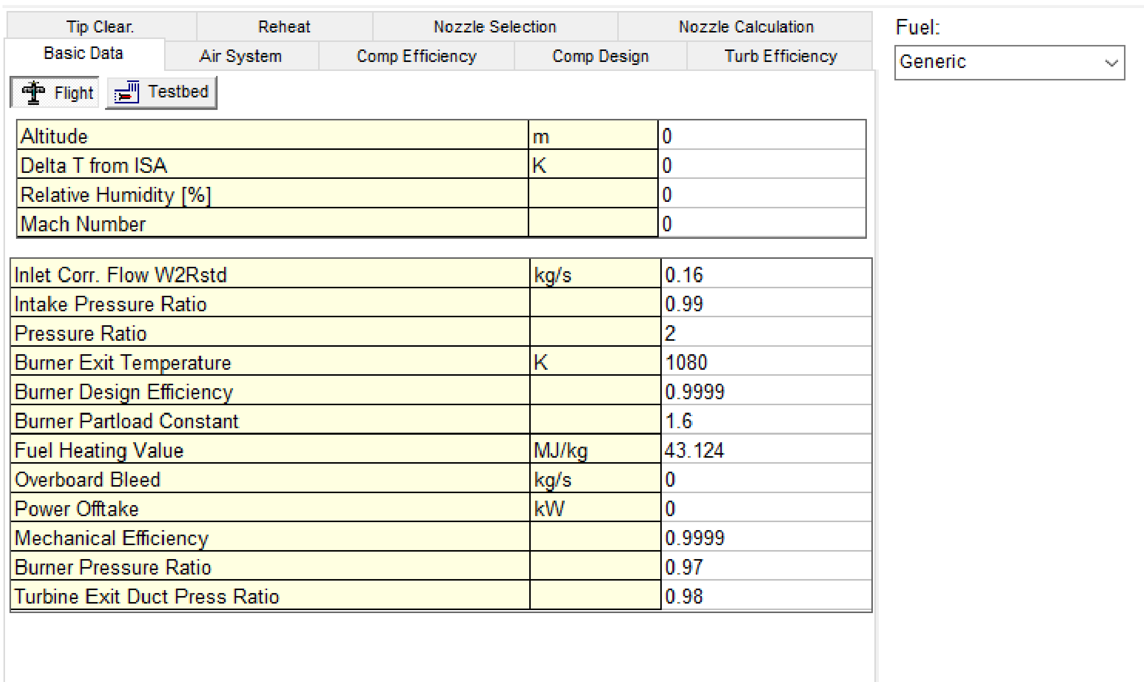

Figure 49. JetCat basic data (generic/propane)

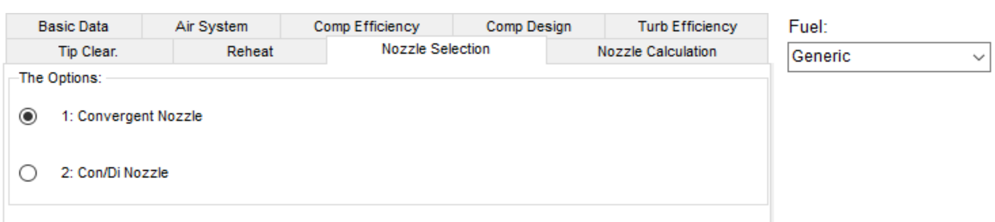

Figure 50. JetCat nozzle selection (generic/propane)

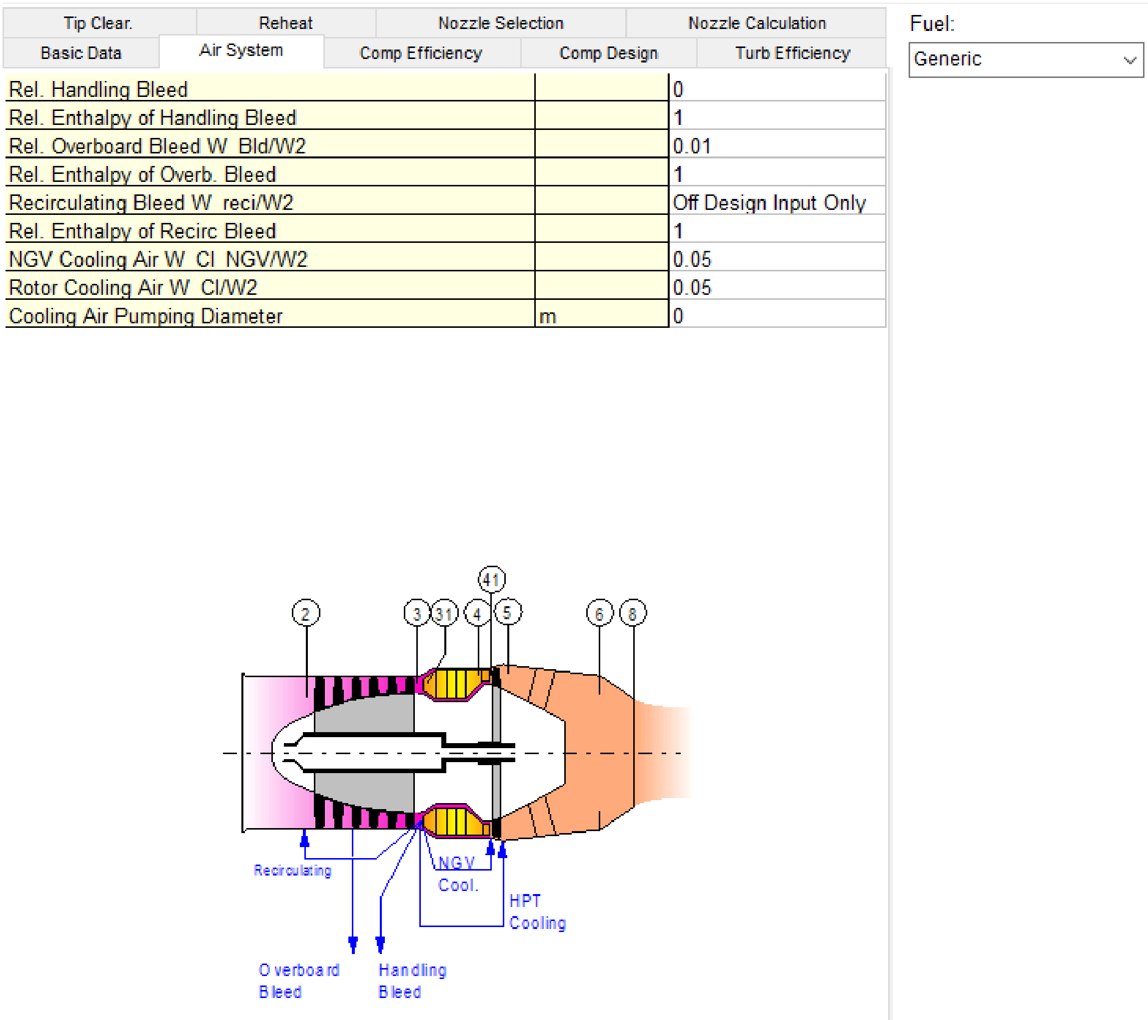

Rel. Handling Bleed		0
Rel. Enthalpy of Handling Bleed		1
Rel. Overboard Bleed W_Bld/W2		0.01
Rel. Enthalpy of Overb. Bleed		1
Recirculating Bleed W_reci/W2		Off Design Input Only
Rel. Enthalpy of Recirc Bleed		1
NGV Cooling Air W_Cl_NGV/W2		0.05
Rotor Cooling Air W_Cl/W2		0.05
Cooling Air Pumping Diameter	m	0

Air system (generic/propane)

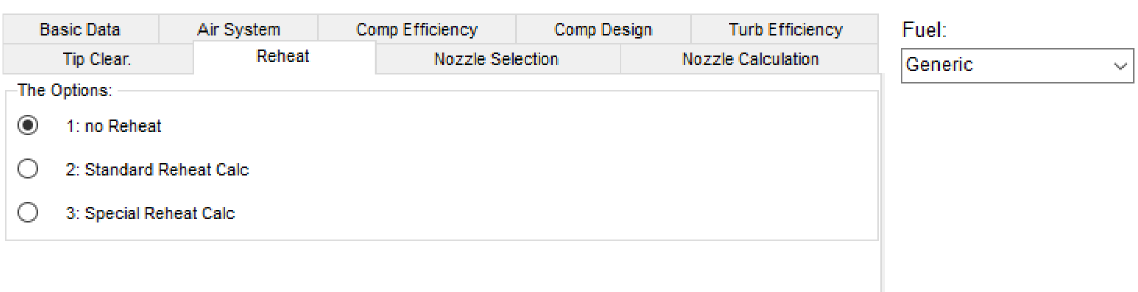

Figure 51. JetCat reheat (generic/propane)

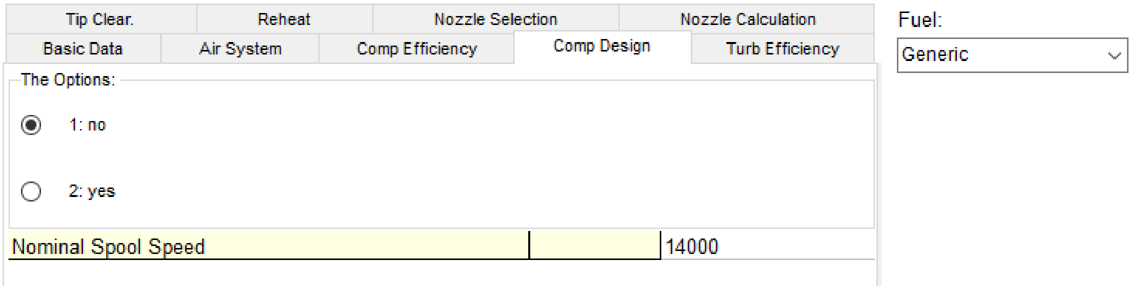

Figure 52. JetCat compressor design (generic/propane)

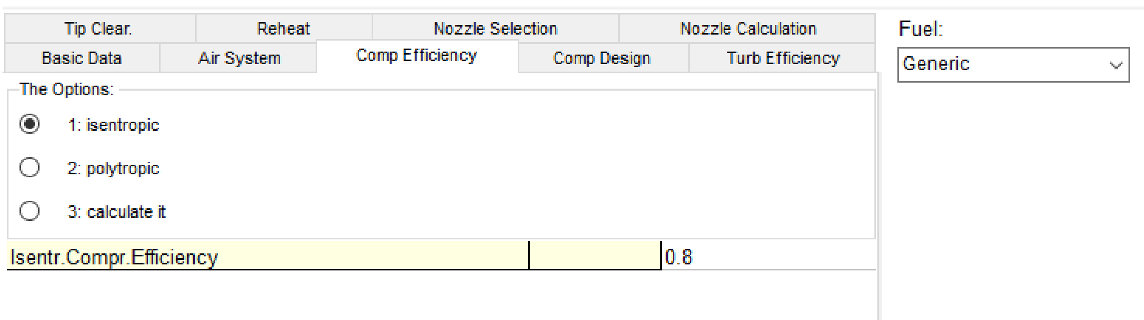

Figure 53. JetCat compressor efficiency (generic/propane)

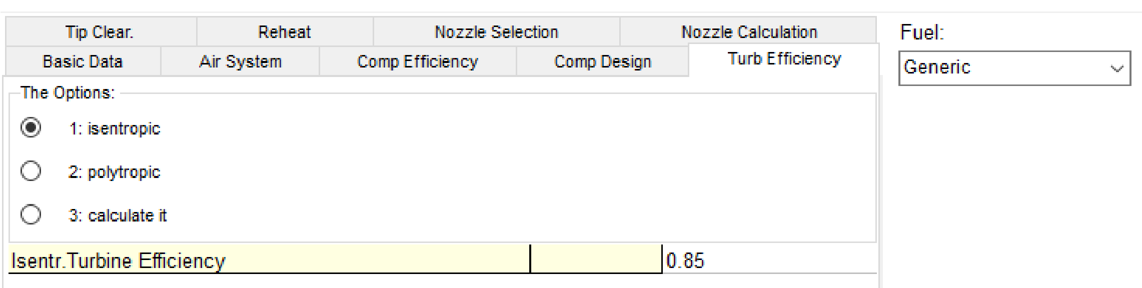

Figure 54. JetCat turbine efficiency (generic/propane)

B. PROPANE OUTPUTS

Summary | Air System

Station	W kg/s	T K	P kPa	WRstd kg/s
amb		288.15	101.325	
1	0.158	288.15	101.325	
2	0.158	288.15	100.312	0.160
3	0.158	366.81	200.624	0.090
31	0.141	366.81	200.624	
4	0.144	1080.00	194.605	0.145
41	0.152	1045.96	194.605	0.150
49	0.152	975.47	138.767	
5	0.159	947.62	138.767	0.211
6	0.159	947.62	135.992	
8	0.159	947.62	135.992	0.215
Bleed	0.002	366.81	200.624	

P2/P1 = 0.9900   P4/P3 = 0.9700   P6/P5 0.9800

Efficiencies:	isentr	polytr	RNI	P/P
Compressor	0.8000	0.8184	0.990	2.000
Burner	0.9999			0.970
Turbine	0.8500	0.8446	0.422	1.402

Spool mech Eff 0.9999   Nom Spd 14000 rpm

hum [%]	war0	FHV	Fuel
0.0	0.00000	43.124	Generic

FN	=	0.06 kN
TSFC	=	42.0655 g/(kN*s)
FN/W2	=	395.58 m/s
Prop Eff	=	0.0000
eta core	=	0.1155
WF	=	0.00264 kg/s
s NOx	=	0.03606
XM8	=	0.6763
A8	=	0.0011 m²
P8/Pamb	=	1.3421
WBld/W2	=	0.01000
Ang8	=	20.00 °
CD8	=	0.9167
W_NGV/W2	=	0.05000
WCL/W2	=	0.05000
Loading	=	100.00 %
e45 th	=	0.83485
far7	=	0.01681
PWX	=	0.00 kW

Figure 55. JetCat summary of outputs (generic/propane)

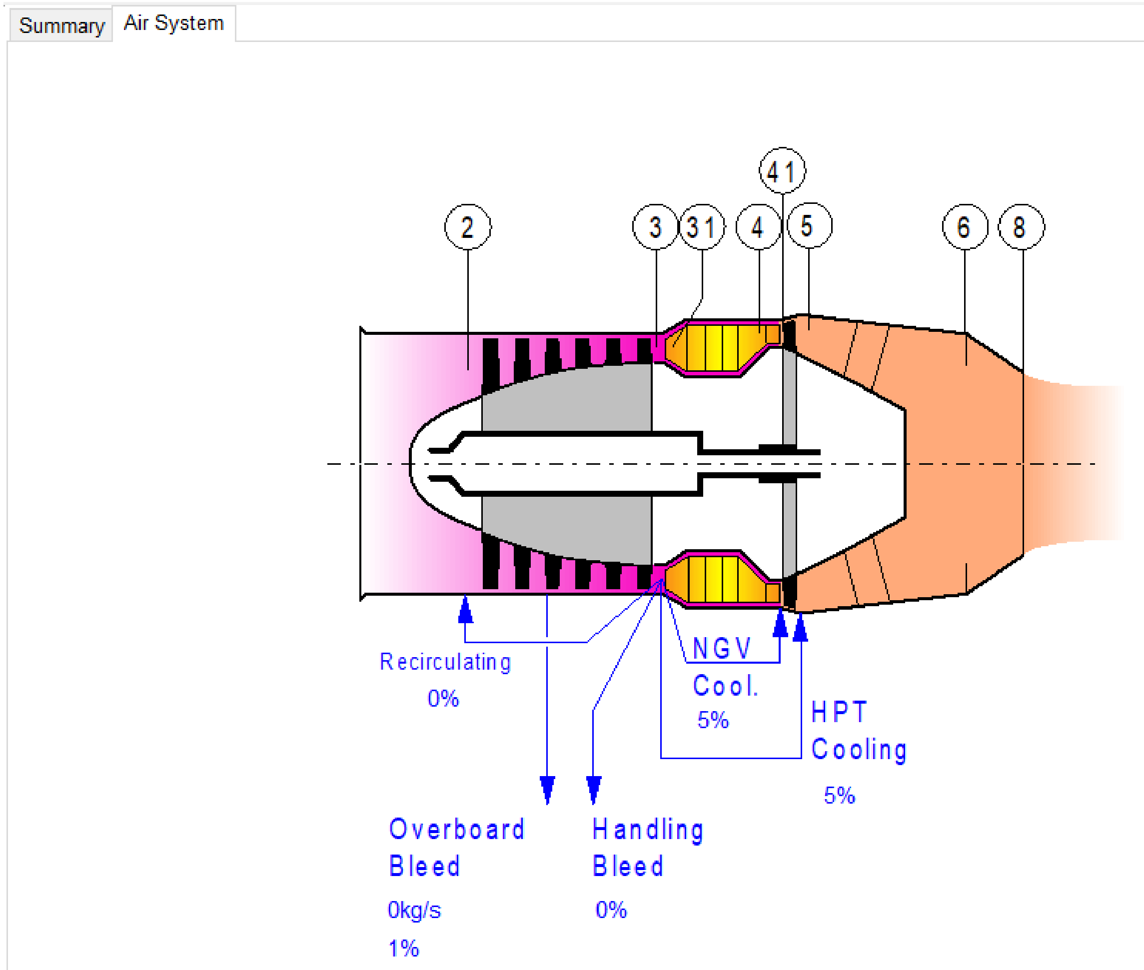

Figure 56. JetCat air system outputs (generic/propane)

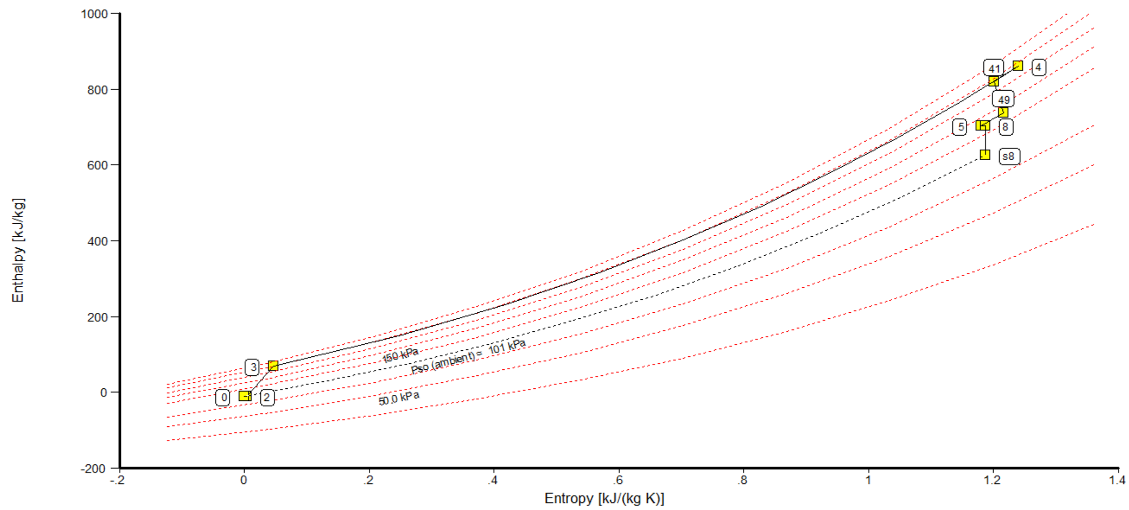

Figure 57. JetCat enthalpy-entropy diagram (generic/propane)

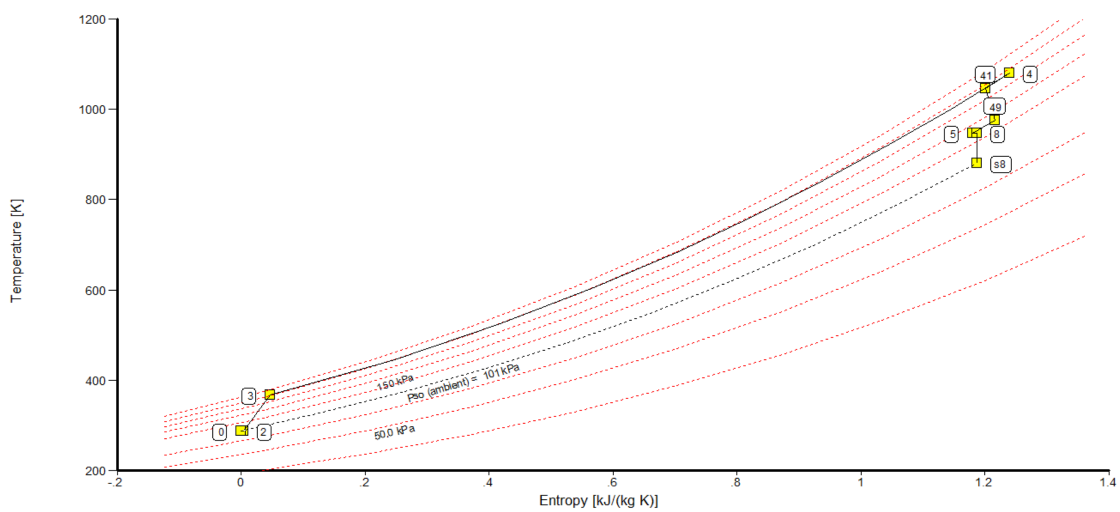

Figure 58. JetCat temperature-entropy diagram (generic/propane)

C. HYDROGEN INPUTS

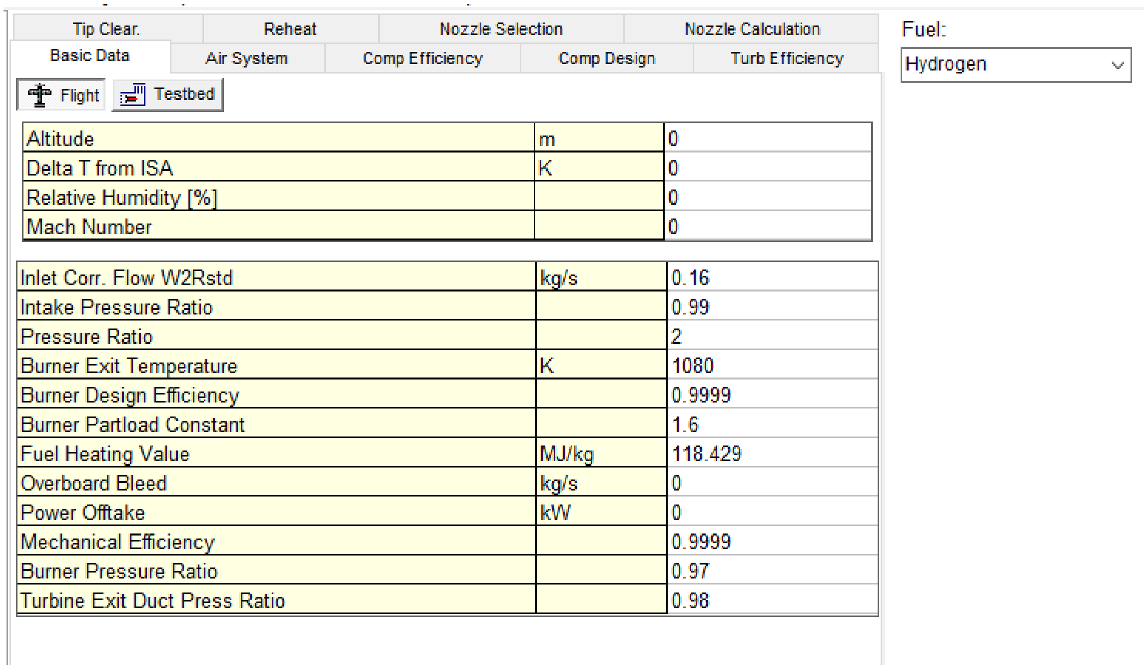

Altitude	m	0
Delta T from ISA	K	0
Relative Humidity [%]		0
Mach Number		0

Inlet Corr. Flow W2Rstd	kg/s	0.16
Intake Pressure Ratio		0.99
Pressure Ratio		2
Burner Exit Temperature	K	1080
Burner Design Efficiency		0.9999
Burner Partload Constant		1.6
Fuel Heating Value	MJ/kg	118.429
Overboard Bleed	kg/s	0
Power Offtake	kW	0
Mechanical Efficiency		0.9999
Burner Pressure Ratio		0.97
Turbine Exit Duct Press Ratio		0.98

Figure 59. JetCat basic data (hydrogen)

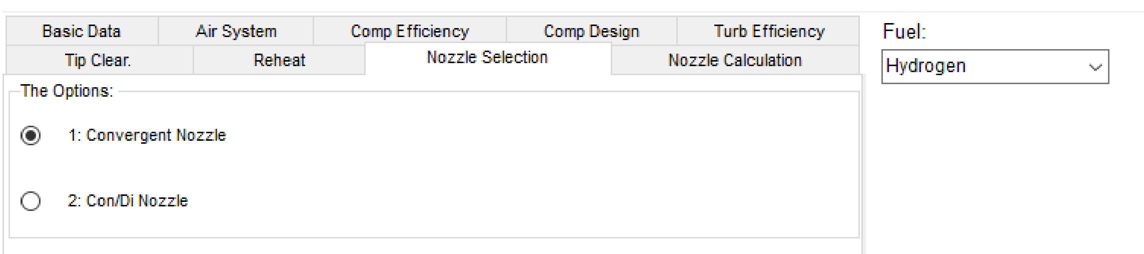

Figure 60. JetCat nozzle selection (hydrogen)

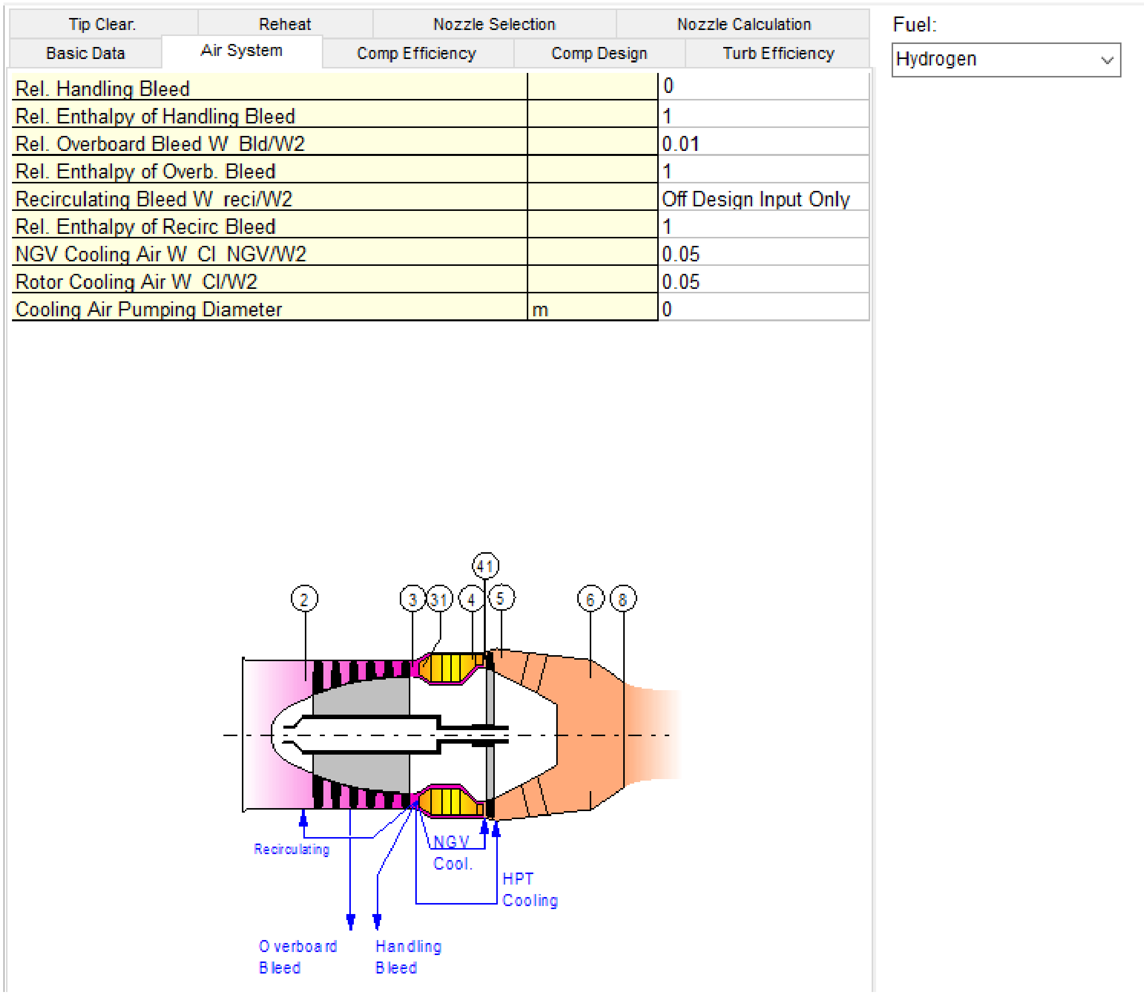

Rel. Handling Bleed		0
Rel. Enthalpy of Handling Bleed		1
Rel. Overboard Bleed W_Bld/W2		0.01
Rel. Enthalpy of Overb. Bleed		1
Recirculating Bleed W_reci/W2		Off Design Input Only
Rel. Enthalpy of Recirc Bleed		1
NGV Cooling Air W_Cl_NGV/W2		0.05
Rotor Cooling Air W_Cl/W2		0.05
Cooling Air Pumping Diameter	m	0

Figure 61. JetCat air system (hydrogen)

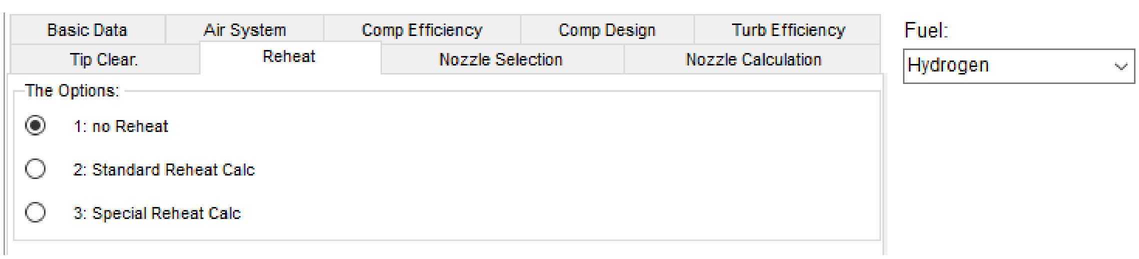

Figure 62. JetCat reheat (hydrogen)

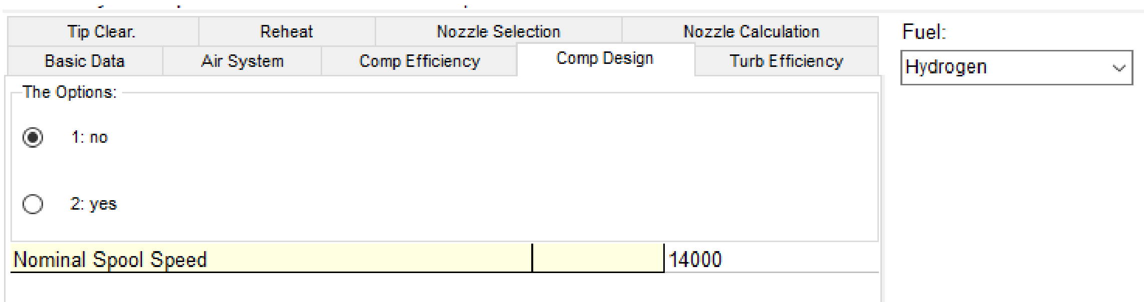

Figure 63. JetCat compressor design (hydrogen)

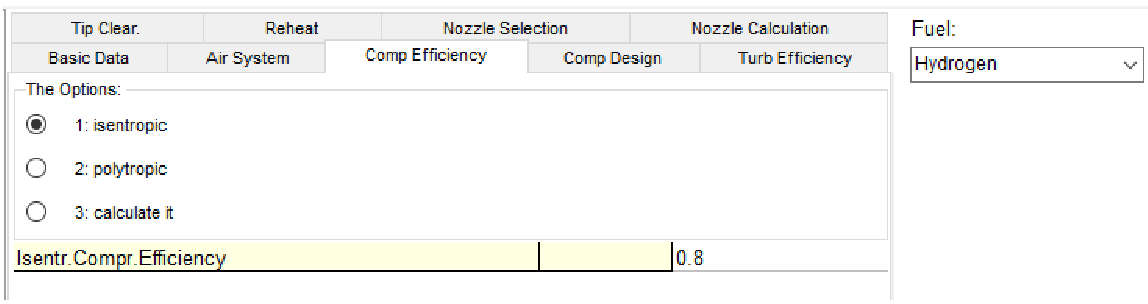

Figure 64. JetCat compressor efficiency (hydrogen)

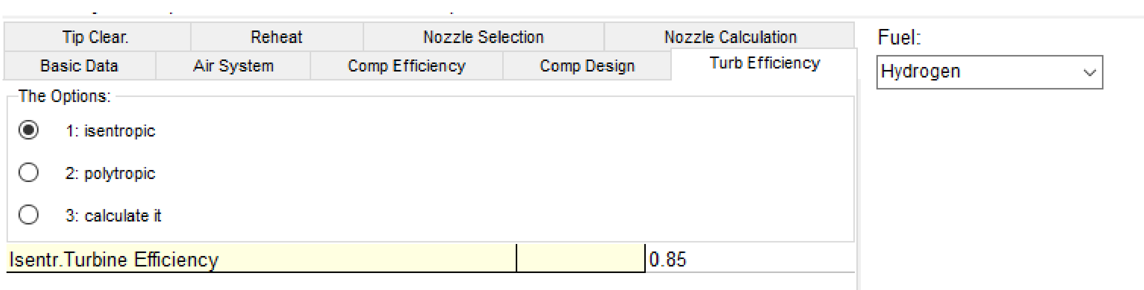

Figure 65. JetCat turbine efficiency (hydrogen)

D. HYROGEN OUTPUTS

Summary | Air System

```
            W          T          P         WRstd
Station  kg/s         K        kPa         kg/s        FN         =       0.06 kN
 amb               288.15    101.325                   TSFC       =    15.1266 g/(kN*s)
  1      0.158     288.15    101.325                   FN/W2      =     406.04 m/s
  2      0.158     288.15    100.312      0.160
  3      0.158     366.81    200.624      0.090        Prop Eff =      0.0000
 31      0.141     366.81    200.624                   eta core =      0.1210
  4      0.142    1080.00    194.605      0.146
 41      0.150    1046.64    194.605      0.151        WF         = 9.7289E-4 kg/s
 49      0.150     977.57    140.193                   s NOx      =    0.03606
  5      0.158     950.14    140.193      0.211        XM8        =     0.6888
  6      0.158     950.14    137.389                   A8         =     0.0011 m²
  8      0.158     950.14    137.389      0.215        P8/Pamb    =     1.3559
Bleed    0.002     366.81    200.624                   WBld/W2    =    0.01000
--------------------------------------------           Ang8       =      20.00 °
P2/P1 = 0.9900  P4/P3 = 0.9700  P6/P5 0.9800           CD8        =     0.9185
Efficiencies:    isentr  polytr     RNI     P/P        W_NGV/W2 =    0.05000
 Compressor      0.8000  0.8184   0.990   2.000        WCL/W2     =    0.05000
 Burner          0.9999                   0.970        Loading    =     100.00 %
 Turbine         0.8500  0.8447   0.422   1.388        e45 th     =    0.83470
--------------------------------------------           far7       =    0.00620
Spool mech Eff   0.9999  Nom Spd     14000 rpm         PWX        =       0.00 kW
--------------------------------------------

hum [%]     war0        FHV      Fuel
   0.0    0.00000    118.429    Hydrogen
```

Figure 66. JetCat summary of outputs (hydrogen)

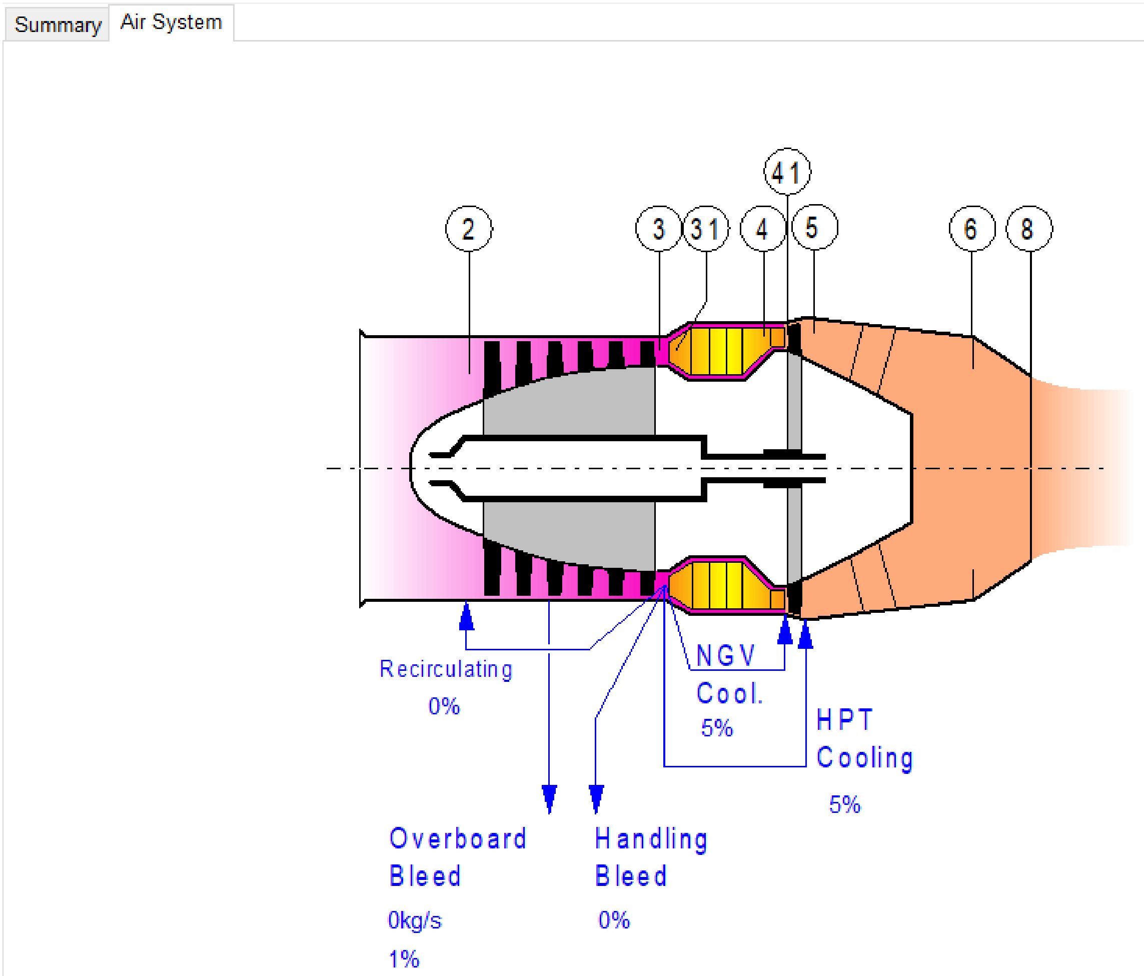

Figure 67. JetCat air system outputs (hydrogen)

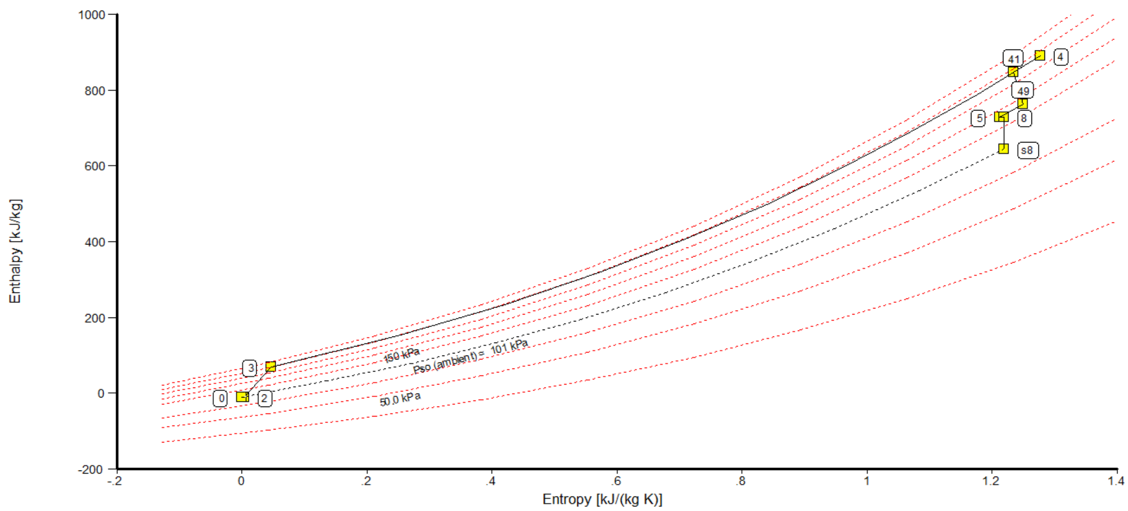

Figure 68. JetCat enthalpy-entropy diagram (hydrogen)

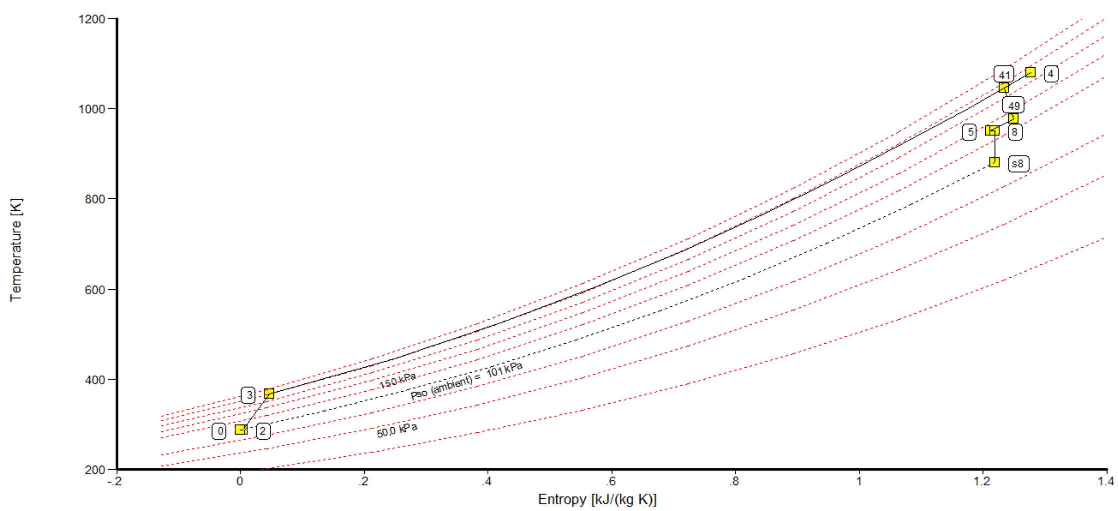

Figure 69. JetCat temperature-entropy diagram (hydrogen)

APPENDIX E. JETCAT BOUNDARY CONDITIONS

The remain boundaries autogenerate by CFX are adiabatic, no slip wall, smooth wall conditions. Ensure the autogenerated boundaries are the desired conditions and that no additional fluid-fluid interfaces were generated when slicing the two solid models.

Table 6. JetCat default domain setup

Domain - Default Domain	
Type	Fluid
Location	B798
Materials	
Hydrogen Air Mixture	
Fluid Definition	Material Library
Morphology	Continuous Fluid
Settings	
Buoyancy Model	Non Buoyant
Domain Motion	Stationary
Reference Pressure	2.0000e+00 [atm]
Combustion Model	Eddy Dissipation
Eddy Dissipation Model Coefficient B	5.0000e-01
Maximum Flame Temperature	2.4000e+03 [K]
Component	H2
Option	Automatic
Component	H2O
Option	Automatic
Component	N2
Option	Constraint
Component	O2
Option	Automatic
Heat Transfer Model	Total Energy
Include Viscous Work Term	True
Turbulence Model	k epsilon
Turbulent Wall Functions	Scalable
High Speed Model	Off
Domain Interface - Trans1	
Boundary List1	Trans1 Side 1
Boundary List2	Trans1 Side 2
Interface Type	Fluid Fluid
Settings	
Interface Models	Rotational Periodicity
Axis Definition	Coordinate Axis
Rotation Axis	Coord 0.2
Mesh Connection	Automatic

Table 7. JetCat inlet boundary conditions

	Boundary - Inlet
Type	INLET
Location	Inlet
	Settings
Component	H2
Mass Fraction	0.0000e+00
Option	Mass Fraction
Component	H2O
Mass Fraction	0.0000e+00
Option	Mass Fraction
Component	O2
Mass Fraction	2.3200e-01
Option	Mass Fraction
Flow Direction	Normal to Boundary Condition
Flow Regime	Subsonic
Heat Transfer	Static Temperature
Static Temperature	3.0000e+02 [K]
Mass And Momentum	Mass Flow Rate
Mass Flow Rate	2.6600e-02 [kg s^-1]
Mass Flow Rate Area	As Specified
Turbulence	Medium Intensity and Eddy Viscosity Ratio

Table 8. JetCat fuel inlet boundary conditions

	Boundary - Fuelin
Type	INLET
Location	Fuelin
	Settings
Component	H2
Mass Fraction	1.0000e+00
Option	Mass Fraction
Component	H2O
Mass Fraction	0.0000e+00
Option	Mass Fraction
Component	O2
Mass Fraction	0.0000e+00
Option	Mass Fraction
Flow Direction	Normal to Boundary Condition
Flow Regime	Subsonic
Heat Transfer	Static Temperature
Static Temperature	3.0000e+02 [K]
Mass And Momentum	Mass Flow Rate
Mass Flow Rate	1.6200e-04 [kg s^-1]
Mass Flow Rate Area	As Specified
Turbulence	Medium Intensity and Eddy Viscosity Ratio

Table 9. JetCat outlet boundary conditions

	Boundary - Outlet
Type	OUTLET
Location	Outlet
	Settings
Flow Regime	Subsonic
Mass And Momentum	Average Static Pressure
Pressure Profile Blend	5.0000e-02
Relative Pressure	-6.0000e-02 [atm]
Pressure Averaging	Average Over Whole Outlet

Table 10. JetCat domain interface boundary conditions

	Boundary - Trans1 Side 1
Type	INTERFACE
Location	Sym1
	Settings
Component	H2
Option	Conservative Interface Flux
Component	H2O
Option	Conservative Interface Flux
Component	O2
Option	Conservative Interface Flux
Heat Transfer	Conservative Interface Flux
Mass And Momentum	Conservative Interface Flux
Turbulence	Conservative Interface Flux
	Boundary - Trans1 Side 2
Type	INTERFACE
Location	Sym2
	Settings
Component	H2
Option	Conservative Interface Flux
Component	H2O
Option	Conservative Interface Flux
Component	O2
Option	Conservative Interface Flux
Heat Transfer	Conservative Interface Flux
Mass And Momentum	Conservative Interface Flux
Turbulence	Conservative Interface Flux

THIS PAGE IS INTENTIONALLY LEFT BLANK

APPENDIX F. JETCAT CFX RESIDUALS

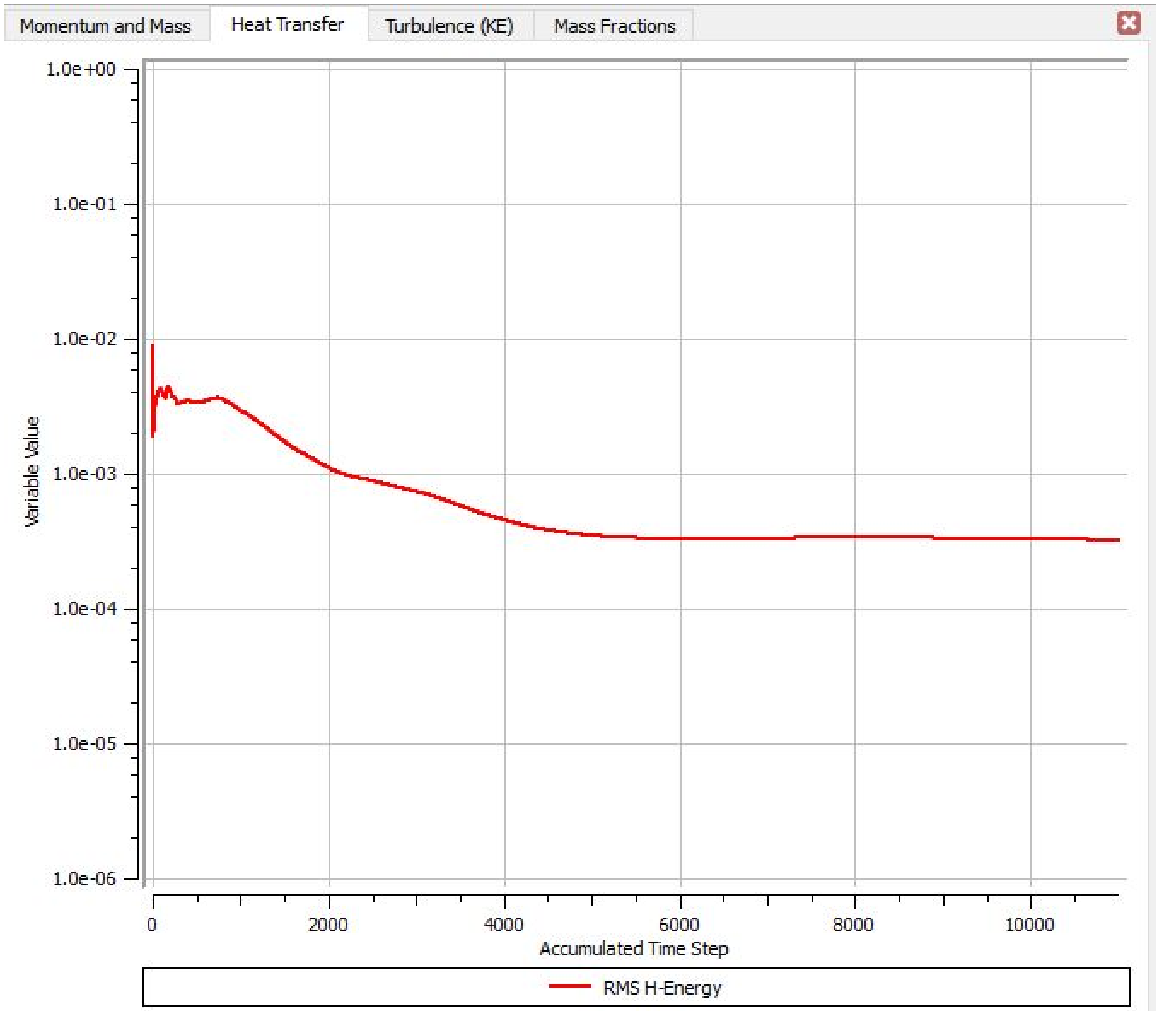

Figure 70. JetCat heat transfer residual

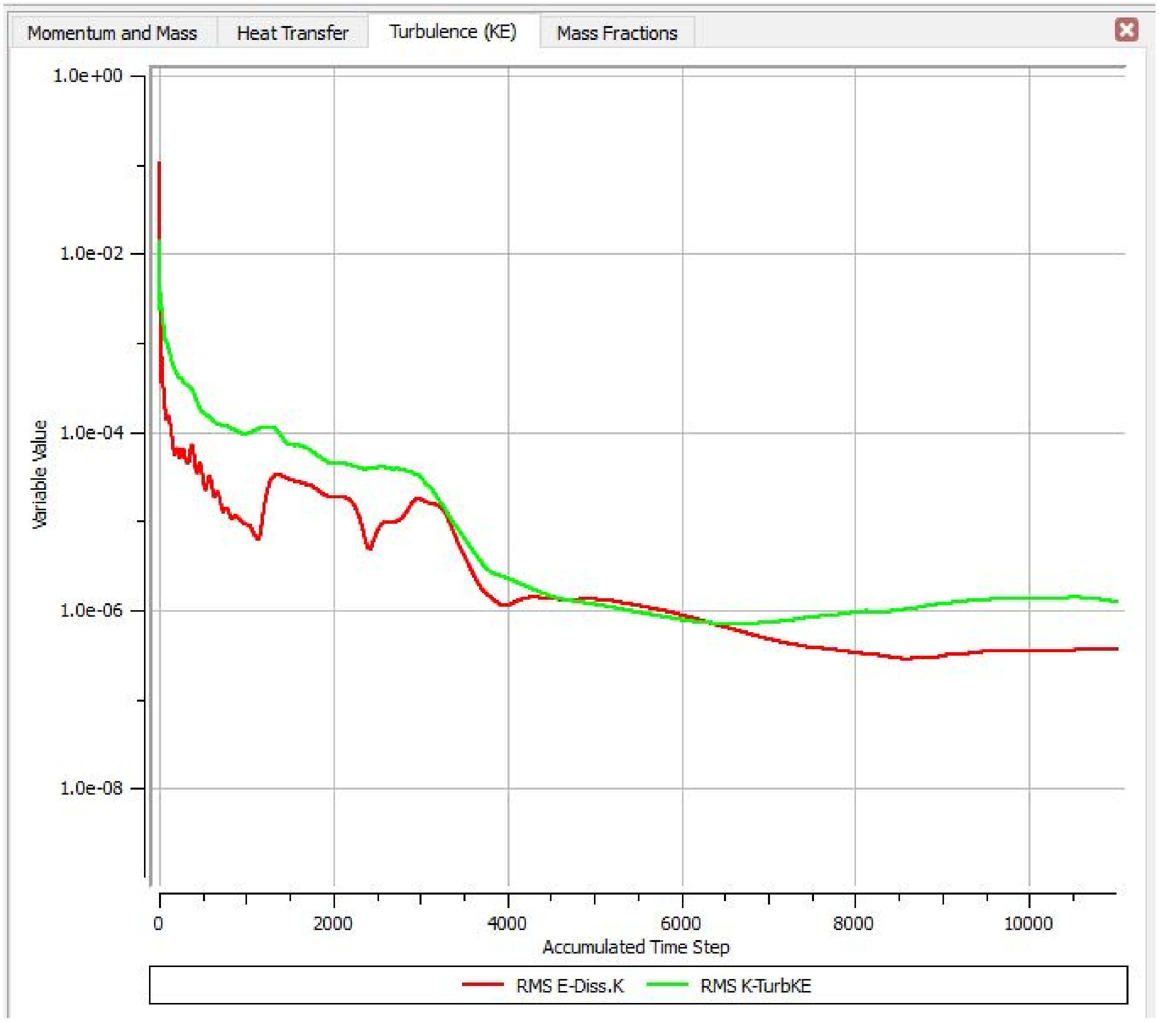

Figure 71. JetCat turbulence residuals

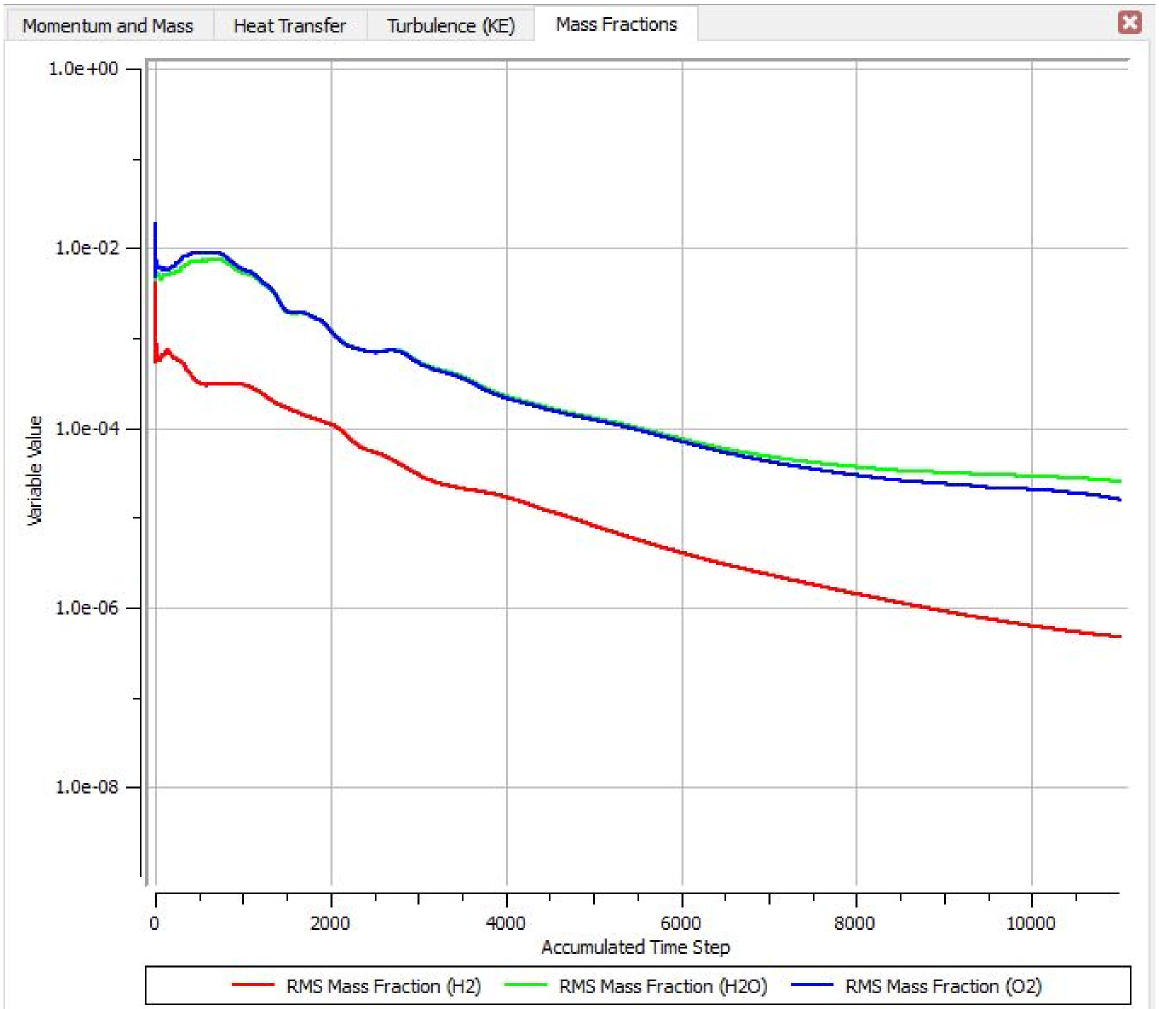

Figure 72. JetCat mass fractions residuals

THIS PAGE IS INTENTIONALLY LEFT BLANK

LIST OF REFERENCES

[1] Assistant Secretary of the Navy Energy Office, “Department of the Navy: Strategy for Renewable Energy,” Washington, DC, USA, 2012. [Online] Available: http://www.secnav.navy.mil/eie/Documents/DoNStrategyforRenewableEnergy.pdf

[2] Assistant Secretary of the Navy Energy Office, “Department of the Navy: Energy Program for Security and Independence,” Washington, DC, USA, 2010. [Online] Available: https://www.secnav.navy.mil/eie/Documents/DoNEnergyProgramforSecurityandIndependence.pdf

[3] Dr. Jeff Waksman, “Project Pele, Mobile Nuclear Power for Future DoD Needs,” presented at the Naval Postgraduate School, Monterey, CA, USA, Mar. 18, 2021. [Online] Available: https://nps.edu/web/nps-video-portal/-/project-pele-mobile-nuclear-power-for-future-dod-needs

[4] U.S. Department of Energy, “Alternative Fuels Data Center: Hydrogen Production and Distribution.” [Online] Available: https://afdc.energy.gov/fuels/hydrogen_production.html

[5] K. Mazloomi, and C. Gomes, “Hydrogen as an energy carrier: Prospects and challenges,” Electrical and Electronic Egr. Dept., University of Putra Malaysia, Selangor, Malaysia 2012. [Online] Available: https://www-sciencedirect-com.libproxy.nps.edu/science/article/pii/S1364032112001220?via%3Dihub

[6] B. Kaufmann, “Implementation of a microturbine in a hydrogen energy storage and generation system,” M.S. thesis, Mech. Egr. Dept., Naval Postgraduate School, Monterey, CA, USA 2019. [Online] Available: https://calhoun.nps.edu/handle/10945/62733

[7] R. Hu, private communication, Feb. 2021.

[8] *X30S-B Load Bank Operation and Service Manual*, Mosebach Manufacturing Company. Pittsburgh, PA, 2017. [Online] Available: https://mosebachresistors.com/support/manuals

[9] Grabcad Community, Santiago. “Combustion Chamber.” February 21, 2014. Accessed October 7, 2020. [Online] Available: https://grabcad.com/library/combustion-chamber-3

[10] *ANSYS CFX Tutorials,* 16th ed. ANSYS, Canonsburg, PA, USA, 2013.

[11] *400001-001 Rev. C: Capstone MicroTurbine User’s Manual*, Capstone Turbine Corporation, Chatsworth, CA, USA, 2005.

[12] *410028 Rev D: Stand Alone Operation – Capstone Model C30 and C60/C65*, Capstone Turbine Corporation, Chatsworth, CA, USA, 2006.

[13] *410013 Rev U: Capstone Remote Monitoring System (User Edition)*, Capstone Turbine Corporation, Chatsworth, CA, USA, 2017.

INITIAL DISTRIBUTION LIST

1. Defense Technical Information Center
   Ft. Belvoir, Virginia

2. Dudley Knox Library
   Naval Postgraduate School
   Monterey, California